ON THE CENTRIFUGAL INSTABILITY OF NONAXISYMMETRIC FLOWS

by

JEFFREY R. KROLL

M.A., University of Nebraska at Omaha, 1970

B.S., Stevens Institute of Technology, 1965

SUBMITTED IN PARTIAL FULFILLMENT OF THE REQUIREMENTS FOR THE DEGREE OF MASTER OF SCIENCE

at the

MASSACHUSETTS INSTITUTE OF TECHNOLOGY

May, 1974

Signature of Author.....
Department of Meteorology, May 1974

Certified by.....
Thesis Supervisor

Accepted by.....
Chairman, Departmental Committee on Graduate Students

ON THE CENTRIFUGAL INSTABILITY OF NONAXISYMMETRIC FLOWS

by

JEFFREY R. KROLL

Submitted to the Department of Meteorology on 9 May 1974 in partial fulfillment of the requirements for the degree of Master of Science.

ABSTRACT

A set of linearized equations for a 2-layer rigid lid model is developed, which is used to investigate the centrifugal instability of nonaxisymmetric flows. A basic state is derived which is stationary, essentially barotropic and stable to Rayleigh (inflection point) instabilities.

A theoretical discussion of the linearized equations, in natural coordinates, reveals the importance of the stability criterion for axisymmetric flows in determining the stability of nonaxisymmetric flows. Additional terms, related to the confluence and difluence of the streamlines, are shown and their possible effect on the flow is discussed.

When the linearized equations are integrated numerically, the form of the instability is seen. The growth rate of the instability is correlated with the criterion for an axisymmetric vortex, but the terms introduced by the asymmetries have a definite destabilizing effect.

Thesis Supervisor: Jule G. Charney

Title: Sloan Professor of Meteorology

ACKNOWLEDGEMENTS

The author wishes to thank his advisor Professor Charney for his advice during the course of this investigation. Thanks are also due to Professor N. A. Phillips who served as an advisor during Professor Charney's absence.

The author would also like to thank his fellow students for the many stimulating discussions from which he learned much.

Thanks are also extended to Susan Wiseman for her efficient typing of the manuscript.

Lastly, he wishes to thank his wife Dorothy for her patience and understanding during his years as a student, to his son David for being a cheerful alarm clock early in the morning and to F.T.D. for his warm greetings in the evening.

TABLE OF CONTENTS

LIST OF FIGURES

I. INTRODUCTION

The centrifugal stability of a rotating balanced flow has a long and extensive history going back to Rayleigh and Helmholtz. The basic idea is that a flow which has a balance between the Coriolis and pressure gradient forces may be unstable if the shear of the velocity is larger than the Coriolis parameter. The most interesting aspects of this type of instability are: 1) the velocity profile need only be linear, in contrast with other flow instabilities which require inflection points and 2) the instability is exactly analogous to the gravitational stability of a particle in hydrostatic balance, which is displaced vertically. There is an extensive literature on the stability of the circular vortex including centrifugal stability and we refer the reader to Charney (1973) for a complete discussion and bibliography.

Our purpose here is to investigate the extent to which the stability criterion for an axisymmetric circular vortex applies to non-axisymmetric flows. To do this, we shall develop a numerical model and analyze the results of several experiments. In Chapter II, we discuss the limitations of a 1-layer model and the suitability of a 2-layer model for this task.

We then show in Chapter III how a steady, almost barotropic basic state can be derived for our model. We find

that in order to meet the requirement of steady flow, the condition on the functional form of the stream function Ψ is that one must be able to write $\nabla^2\Psi = G(\Psi)$. This limits the types of flow patterns one can use.

The use and limitations of integrating the nonlinear equations is discussed in Chapter IV and a linearized set of equations is derived for both the barotropic and baroclinic modes. The Rayleigh (inflection point) instability of the barotropic mode is investigated and the streamfunctions which we shall use are found to be stable. This is important because we must be sure of which stability problem we are investigating. We have eliminated the possible baroclinic instabilities by choosing a basic state which is nearly barotropic and, as stated above, we have eliminated the Rayleigh type of instability.

In Chapter V, we discuss the meaning of the stability criterion for a circular vortex. The perturbation equations developed in Chapter IV are in Cartesian coordinates, which do not explicitly show the important terms analogous to the circular vortex. We therefore recast our perturbation equations in terms of the natural coordinates of the flow, defined by the streamlines of the basic state. In this form, we can readily see the terms which are associated with the stability of the circular vortex and additional terms which are due to the nonaxisymmetric nature of the flow. We then discuss

possible modifications of the stability criterion due to these terms.

The results of our numerical experiments are presented in Chapter VI. We see one important result is that the perturbation is strongest in a region of strong anticyclonic curvature and the wave fronts line up perpendicular to rather than along the streamlines of the basic state. The growth rate of the perturbation increases in the direction the classical criterion predicts but we are unable to give a good quantitative prediction based on the present theory. In fact, we show several cases where we expect no growth but in fact the perturbation energy does grow in time. These and other results are discussed in detail in Chapter VII.

II. DERIVATION OF MODEL EQUATIONS

In order to study the centrifugal instability of non-axisymmetric flows, we can choose among several possible models. The simplest model is the one layer, homogeneous shallow water model on an f-plane. If we consider the stability of a basic state $\bar{u}(y)$ which is in geostrophic balance with the gradient of the free surface height $\bar{h}(y)$, we can easily show by a local stability analysis that the condition for centrifugal instability is

$$gHk^2 + f(f - \bar{u}_y) < 0 \qquad (2.1)$$

where k is the wave number in the y direction and H is the mean depth of the fluid. It happens that for any linear velocity profile $\bar{u} = u_0 y$ such that Eqn 2.1 holds, the flow is stable. The reason for this contradiction is that the linearization is incorrect. On cannot neglect the y variation of the free surface. Physically, we require the angular momentum to decrease in the negative y direction (assuming y is positive toward the north). The product of the mass times the velocity should increase as y increases, but the free surface $\bar{h}(y)$ decreases so rapidly toward increasing y that, even though the velocity $\bar{u}$ increases, the product $\bar{h}(y)\bar{u}(y)$ decreases. For this reason the one layer model is not suitable. The main consideration is to allow another degree of freedom which minimizes the above

effect. This can be achieved by a continuously stratified model or an n-layer model. As discussed by Houghton and Young (1970), the continuous model provides for the minimization of the stabilizing effect of gravity by allowing very short vertical wavelengths.

An alternate approach is to use an n-layer model, the simplest being a two-layer model. In this model the gravitationally stabilizing term is minimized by the reduced gravity entering the stability analysis rather than g itself and the variation in the free surface and interface heights is negligible thus making the local analysis valid. The geometry of the model is shown in Fig. 1.1. We have a re-entrant channel in the x-direction, lateral boundaries at $y = 0$ and $y = w$, a flat bottom and a rigid lid. We assume we are on an f-plane, far from the axis of rotation, so that Cartesian coordinates can be used.

In the vertical, we have two layers of slightly different densities ρ_1 in the upper and ρ_2 in the lower. We assume that the system is gravitationally stable so that $\rho_1 < \rho_2$. The constraint of a rigid lid introduces a reaction pressure p on the upper layer. The equations of motion for this two layer model can be written

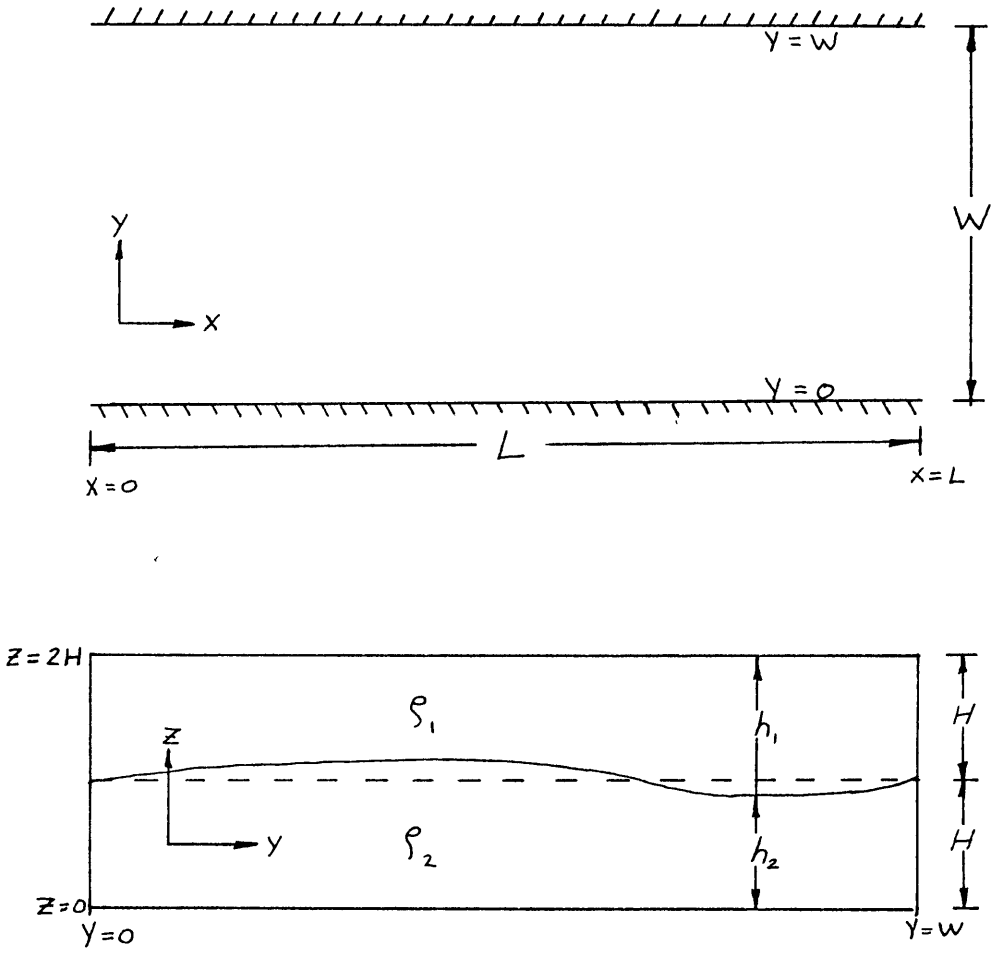

Fig. 1.1 Physical geometry of the model.

$$\frac{du_i}{dt} - fv_i = -\frac{1}{\rho_i}\frac{\partial p}{\partial x} - \delta_{i2}\frac{(\rho_2-\rho_1)}{\rho_2} g \frac{\partial h_2}{\partial x}$$

$$\frac{dv_i}{dt} + fu_i = -\frac{1}{\rho_i}\frac{\partial p}{\partial y} - \delta_{i2}\frac{(\rho_2-\rho_1)}{\rho_2} g \frac{\partial h_2}{\partial x} \qquad (2.2)$$

$$\frac{dh_i}{dt} + h_i \nabla\cdot\mathbf{V}_i = 0$$

where i = 1, 2, $\frac{d}{dt} = \frac{\partial}{\partial t} + \mathbf{V}_i\cdot\nabla$,

δ_{i2} is the Kronecker delta, $h_1 = 2H - h_2$ and p is the pressure in the upper layer.

We nondimensionalize the above equations in the following manner:

$$\begin{aligned} u_i, v_i &\longrightarrow U u_i, U v_i \\ x, y &\longrightarrow Lx, Ly \\ t &\longrightarrow f^{-1}t \\ h_i &\longrightarrow H(1+\varepsilon R_o h_i) \\ p &\longrightarrow (\rho_1 f U L)p \end{aligned} \qquad (2.3)$$

where $\varepsilon = \frac{f^2L^2}{g'H}$, $R_o = \frac{U}{fL}$, $g' = (1-\gamma)g$, $\gamma = \frac{\rho_1}{\rho_2}$

and H is the mean depth of each layer. The equations of motion then become

$$\frac{du_i}{dt} - v_i = -\gamma_i\frac{\partial p}{\partial x} - \delta_{i2}\frac{\partial h_2}{\partial x}$$

$$\frac{dv_i}{dt} + u_i = -\gamma_i\frac{\partial p}{\partial y} - \delta_{i2}\frac{\partial h_2}{\partial y} \qquad (2.4)$$

$$\frac{dh}{dt} + \frac{1}{\varepsilon}(1+\varepsilon R_o h_i)\nabla\cdot\mathbf{V}_i = 0$$

where $\gamma_1 = 1$, $\gamma_2 = \gamma$, $\frac{d}{dt} = \frac{\partial}{\partial t} + R_o \mathbf{V}_i \cdot \nabla$.

If one wishes to integrate the full set of nonlinear equations (Eqs 2.4), it is convenient to write the momentum and continuity equations in flux form. To do this, we define the total scaled depth of each layer: $d_i = 1 + \varepsilon R_o h_i$. Eqs 2.4 then become

$$\frac{\partial U_i}{\partial t} + R_o \frac{\partial}{\partial x} u_i U_i + R_o \frac{\partial}{\partial y} u_i V_i - V_i = -\gamma_i d_i \frac{\partial P}{\partial x} - \frac{\delta_{i2}}{2\varepsilon R_o} \frac{\partial d_2^2}{\partial x}$$

$$\frac{\partial V_i}{\partial t} + R_o \frac{\partial}{\partial x} v_i U_i + R_o \frac{\partial}{\partial y} v_i V_i + U_i = -\gamma_i d_i \frac{\partial P}{\partial y} - \frac{\delta_{i2}}{2\varepsilon R_o} \frac{\partial d_2^2}{\partial y}$$

$$\frac{\partial}{\partial t} d_i + R_o \frac{\partial U_i}{\partial x} + R_o \frac{\partial V_i}{\partial y} = 0$$

where $U_i = d_i u_i$ and $V_i = d_i v_i$. Note that the constraint of a rigid lid implies that $d_1 + d_2$ = constant, i.e., $h_1 = -h_2$, thus $d_1 + d_2 = 2$. Therefore we need to integrate only one continuity equation. A method for integrating Eqs 2.4 is discussed by Lilly (1965) and the procedure for maintaining the constraint of the rigid lid is discussed by Smagorinsky (1958).

III. THE BASIC STATE

In order to study the centrifugal instability of curved flow, we must be certain that other types of instabilities are not possible for our basic state. In order to ensure that we do not have baroclinic instability, we would like our basic state to be as close to barotropic as possible. We must also be certain that our basic state is stable to purely horizontal perturbations of the Rayleigh type of instability.

We must find a (nearly) barotropic non-axisymmetric flow which satisfies the equations of motion and then either integrate the nonlinear Eqs. 2.5 to see if a small random perturbation grows or else linearize about that basic state and again consider the growth of a small perturbation. In either case, it is desirable to find a stationary basic state.

We begin by noting that, for each layer, the steady-state momentum and continuity equations may be combined to give the potential vorticity equation

$$\mathbf{V}_i \cdot \nabla \left(\frac{R_o \zeta_i + 1}{d_i} \right) = 0 \tag{3.1a}$$

If we assume that $\mathbf{V}_i$ is nondivergent, we can write

$$\mathbf{V}_i = \hat{k} \times \nabla \psi_i \tag{3.1b}$$

and

$$\zeta_i = \nabla^2 \psi_i \tag{3.1c}$$

The steady-state continuity equation therefore is

$$(\mathbb{V}_i \cdot \nabla)\, d_i = 0 \quad . \tag{3.1d}$$

If Eqn 3.1a is to hold, $\frac{R_o \mathcal{F}_i + 1}{d_i} = F(\Psi_i)$ because $\mathbb{V}_i$ is perpendicular to $\nabla \Psi_i$. Eqn 3.1d implies that $d_i = d_i(\Psi_i)$ and therefore $R_o \mathcal{F}_i + 1$ must also be a function of Ψ_i . One can rewrite the momentum Eqs 2.4 for each layer

$$R_o \nabla \frac{(\nabla \Psi_i)^2}{2} - (R_o \mathcal{F}_i + 1) \nabla \Psi_i = -\gamma_i \nabla \mathcal{P} - \delta_{i2} \nabla h_2 \tag{3.2}$$

and since $R_o \mathcal{F}_i + 1$ is a function of Ψ_i ,

$$(R_o \mathcal{F}_i + 1) \nabla \Psi_i = \nabla G_i(\Psi_i) \tag{3.3}$$

Eqn 3.2 then gives

$$\gamma_i \mathcal{P} + \delta_{i2} h_2 = G_i(\Psi_i) - R_o \frac{(\nabla \Psi_i)^2}{2} \quad . \tag{3.4}$$

Taking γ times Eqn 3.4 with i = 1 and subtracting from Eqn 3.4 with i = 2 gives

$$h_2 = G_2(\Psi_2) - \gamma G_1(\Psi_1) - \frac{R_o}{2}\left[(\nabla \Psi_1)^2 - \gamma (\nabla \Psi_2)^2\right] \tag{3.5}$$

From Eqn 3.5, we see that h_2 is a function of Ψ_2 only if $\Psi_2 = \gamma^{1/2} \Psi_1$. In this case we have

$$h_2 = G_2(\Psi_2) - \gamma G_1(\gamma^{-1/2} \Psi_2) \quad . \tag{3.6}$$

One can easily show from Eqs 3.3 and 3.6 that $h_2 = \gamma^{1/2}(1-\gamma^{1/2})\psi_1 = (1-\gamma^{1/2})\psi_2$ plus a constant which is independent of x and y. Thus $d_2 = 1 + \varepsilon R_o h_2$ satisfies Eqn 3.1d and $d_1 = 1 + \varepsilon R_o h_1 = 1 - \varepsilon R_o h_2$ also satisfies Eqn 3.1d.

Note that the rigid lid provides a reaction pressure which filters out the bothersome barotropic gravity wave in the numerical computations.

To summarize the conditions on the flow, we write them as follows:

$$\frac{\partial G}{\partial \psi} = R_o \nabla^2 \psi + 1 \tag{3.7a}$$

$$p = G(\psi) - R_o \frac{(\nabla \psi)^2}{2} \tag{3.7b}$$

$$h_2 = \gamma^{1/2}(1-\gamma^{1/2})\,\psi \tag{3.7c}$$

$$V_1 = \hat{k} \times \nabla \psi \tag{3.7d}$$

$$V_2 = \gamma^{1/2} V_1 \tag{3.7e}$$

The purpose of the density difference is to reduce the effective gravity and therefore the gravitational stabilizing effect. Its inertial effect is unimportant if we let $\gamma = \rho_1/\rho_2 \approx 1$, thus $V_2 \approx V_1$ and the flow is essentially barotropic. A measure of the baroclinicity is given by

$$\hat{V} = V_1 - V_2 \tag{3.6}$$

Since $W_2 = \gamma^{1/2} W_1$, $\hat{W} = (1 - \gamma^{1/2}) W_1$. In the cases we will consider in our numerical experiments, $\gamma^{1/2} \doteq .999$, which implies that $\hat{W} \sim O(10^{-3})$ if $W_1 \sim O(1)$. Thus our basic state is nearly barotropic and for our purpose will be considered as such.

We should also note that Eqn 3.7a places a serious constraint on the form of the stream functions which one can choose for stationary flows. For example, a stream function commonly used to represent jet-like flows is $\Psi = -Y + \cos kx * \sin ky$ and therefore $\nabla^2\Psi = -2k^2 \cos kx \sin ky$. One cannot find a function $G(\Psi)$ such that $\frac{\partial G}{\partial \Psi} = \nabla^2\Psi + 1$. One can also show that if Ψ_1 and Ψ_2 are two different stream functions which satisfy Eqn 3.5a separately, neither their sum nor their product do so. As a consequence, in our numerical work we shall use a stream function of the form

$$\Psi = A\left[\cos k_1 (Y - Y_0) + R \sin k_x X \sin k_y Y\right]$$
$$k_1 = (k_x^2 + k_y^2)^{1/2} \qquad (3.8)$$

where A and R are constants to be specified.

We now have

$$\nabla^2\Psi = A\left(-k_1^2 \cos k_1 (Y - Y_0) + R(-k_x^2 - k_y^2) \sin k_x X \sin k_y Y\right)$$
$$= -k_1^2 \Psi$$

and we can specify $G(\Psi)$:

$$G(\Psi) = -\frac{k_1^2}{2} \Psi^2 + \Psi$$

which satisfies Eqn 3.5a.

IV. LINEARIZED EQUATIONS

Having developed a model and a basic state which is unchanging in time, we might be tempted to integrate Eqs 2.4 numerically to determine the stability of this basic state. One could subtract the basic state components from the evolving flow and use the growth of this difference as a measure of the instability. However, there are several shortcomings to this approach. If we wish to study the linear case with a nonlinear model, we must make the initial perturbation small enough to make the nonlinear terms negligible during the entire integration. The finite differencing errors introduce perturbations orders of magnitude larger than one would like to begin with and the nonlinear phase is approached rather quickly.

Fortunately, before we reach the nonlinear phase, another disaster overtakes us - the interface becomes so perturbed that it "hits" the lid and bottom, causing the model to become numerically unstable.

In light of the preceding discussion, we shall linearize Eqs 2.4. Recalling that our basic state is very close to barotropic and that $h_2 << 1$, we shall linearize about the basic state

$$\bar{V}_1 = \bar{V}_2 = \bar{V} \qquad (4.1)$$

$$\bar{h}_1 = \bar{h}_2 = 0$$

We write the velocity and height components as

$$u_i = \bar{u} + \delta u_i'$$
$$v_i = \bar{v} + \delta v_i'$$
$$h_i = \bar{h} + \delta h_i'$$
$$p = \bar{p} + \delta p'$$

where δ is an arbitrarily small parameter, defining the relative size of the perturbation, and the primed quantities are therefore 0(1). The perturbation equations are (dropping the primes):

$$\frac{\partial u_i}{\partial t} + R_o \bar{\mathbb{V}} \cdot \nabla u_i - v_i + \gamma_i \frac{\partial p}{\partial x} + \delta_{i2} \frac{\partial h_2}{\partial x} = -R_o u_i \frac{\partial \bar{u}}{\partial x} - R_o v_i \frac{\partial \bar{u}}{\partial y}$$

$$\frac{\partial v_i}{\partial t} + R_o \bar{\mathbb{V}} \cdot \nabla v_i + u_i + \gamma_i \frac{\partial p}{\partial y} + \delta_{i2} \frac{\partial h_2}{\partial y} = -R_o u_i \frac{\partial \bar{v}}{\partial x} - R_o v_i \frac{\partial \bar{v}}{\partial y} \qquad (4.2)$$

$$\frac{\partial h_i}{\partial t} + R_o \bar{\mathbb{V}} \cdot \nabla h_i + \frac{1}{\varepsilon} \nabla \cdot \mathbb{V}_i = 0$$

We now define $\tilde{\mathbb{V}} = \mathbb{V}_1 + \mathbb{V}_2$ and $\hat{\mathbb{V}} = \mathbb{V}_2 - \gamma \mathbb{V}_1 \approx \mathbb{V}_2 - \mathbb{V}_1$ and recall that $h_1 = -h_2$. We use Eqs 4.2 to obtain equations for the variables $\tilde{\mathbb{V}}$ and $\hat{\mathbb{V}}$:

$$\frac{\partial \tilde{u}}{\partial t} + R_o \bar{\mathbb{V}} \cdot \nabla \tilde{u} - \tilde{v} + (1+\gamma) \frac{\partial p}{\partial x} + \frac{\partial h_2}{\partial x} = -R_o \left[\tilde{u} \frac{\partial \bar{u}}{\partial x} + \tilde{v} \frac{\partial \bar{u}}{\partial y} \right]$$

$$\frac{\partial \tilde{v}}{\partial t} + R_o \bar{\mathbb{V}} \cdot \nabla \tilde{v} + \tilde{u} + (1+\gamma) \frac{\partial p}{\partial y} + \frac{\partial h_2}{\partial y} = -R_o \left[\tilde{u} \frac{\partial \bar{v}}{\partial x} + \bar{v} \frac{\partial \bar{v}}{\partial y} \right]$$

$$\nabla \cdot \tilde{\mathbb{V}} = 0 \qquad (4.3a)$$

and

$$\frac{\partial \hat{u}}{\partial t} + R_o \bar{\mathbb{V}} \cdot \nabla \hat{u} - \hat{v} + \frac{\partial h_2}{\partial x} = -R_o \left[\hat{u} \frac{\partial \bar{u}}{\partial x} + \hat{v} \frac{\partial \bar{u}}{\partial y} \right]$$

$$\frac{\partial \hat{v}}{\partial t} + R_o \bar{\mathbb{V}} \cdot \nabla \hat{v} + \hat{u} + \frac{\partial h_2}{\partial y} = -R_o \left[\hat{u} \frac{\partial \bar{v}}{\partial x} + \hat{v} \frac{\partial \bar{v}}{\partial y} \right] \qquad (4.3b)$$

$$\frac{\partial h_2}{\partial t} + R_o \bar{\mathbb{V}} \cdot \nabla h_2 + \frac{1}{\varepsilon (1+\gamma)} \nabla \cdot \hat{\mathbb{V}} = 0$$

We now have two sets of equations, with the reaction pressure, p , entering only in the first set, Eqs 4.3a. One can immediately recognize Eqs 4.3a as the equations for barotropic nondivergent flow, with a forcing function on the right hand side. If we denote $\bar{\mathbb{V}} = \hat{k} \times \nabla \bar{\Psi}$, $\tilde{\mathbb{V}} = \hat{k} \times \nabla \tilde{\Psi}$, $\bar{\zeta} = \nabla^2 \bar{\Psi}$ and $\zeta' = \nabla^2 \psi'$ we can rewrite 4.3a as

$$\left(\frac{\partial}{\partial t} + R_o \bar{\mathbb{V}} \cdot \nabla \right) \tilde{\zeta} = -R_o \tilde{\mathbb{V}} \cdot \nabla \bar{\zeta} \qquad (4.4)$$

which, in the case of $\bar{\mathbb{V}} = \bar{u}(y)\, \hat{\imath}$, is the classical Rayleigh problem for two dimensional nondivergent parallel flow. In the case of Eqn 4.4, we have the more general

problem of barotropic stability of nonparallel flow. This problem (or ones similar to it) has received some attention over the past several years, notably in papers by Dikii (1965) and Blumen (1968). They assume a functional dependence between $\bar{\psi}$ and $\bar{\zeta}$, i.e., $\bar{\psi} = \bar{\psi}(\bar{\zeta})$ or $\bar{\zeta} = \bar{\zeta}(\bar{\psi})$. This is equivalent to restricting the basic state to be stationary in time, that is $\frac{\partial \bar{\zeta}}{\partial t} \equiv 0$. The method of establishing the stability criterion is a variational principle developed by Arnold (1965). (See Appendix A for a derivation of the criterion for barotropic flow in a channel.) In order to insure stability, the integral

$$\iint \left[(\delta \psi_x)^2 + (\delta \psi_y)^2 + \frac{\partial \bar{\psi}}{\partial \bar{\zeta}} (\delta \bar{\zeta})^2 \right] dx\, dy \qquad (4.5)$$

must be positive definite. This will be so if $\frac{\partial \bar{\psi}}{\partial \bar{\zeta}} \geq 0$ over the entire domain.

It is clear from Chapter III that the basic state we have chosen is indeed steady. However, it is also clear that $\bar{\zeta} = \nabla^2 \bar{\psi}$ gives $\bar{\zeta} = -k_1^2 \bar{\psi}$, and therefore $\frac{\partial \bar{\psi}}{\partial \bar{\zeta}} \leq 0$ everywhere. This does not imply that the flow is unstable, merely that Arnolds sufficient criterion for stability is not satisfied.

The Rayleigh stability criterion for plane parallel flow is that if $\frac{\partial \bar{\zeta}}{\partial y} \neq 0$ everywhere, the flow is stable. By analogy, we might conjecture that if $\frac{\partial \bar{\zeta}}{\partial \bar{\psi}} \neq 0$ everywhere the flow should be stable (See Chapter VII). Here $\bar{\psi}$

is a natural coordinate which takes the place of the cross-stream coordinate y in parallel flow. As a test of the stability of our basic state, we made a numerical experiment using a stream function Ψ of the form of Eqn 3.7. In one experiment R was 2.0 and in another R was 0.0 (purely zonal flow). The wave numbers k_x and k_y were taken to be equal to π/W, W being the width of the channel. y_o was chosen so that in the case R = 0, the maximum of the cosine curve was at mid-channel (Fig. 4.1). We note that the velocity profile has inflection points near the walls and that $\bar{u}$ and $\overline{\zeta}_y$ are positively correlated. Although the necessary conditions for instability were satisfied, when Eqs 4.3a were integrated to more than 20 hours, no instability developed, as evidenced by the graph of total perturbation energy versus time (Fig. 4.2). Similar results were obtained for the case R = 2.0. Apparently the inflection points were so close to the walls that the walls prevented the instability from occurring.

It follows from our considerations that if we now attempt to integrate Eqs 4.3b we shall be studying the centrifugal instability of the flow and not the barotropic instability.

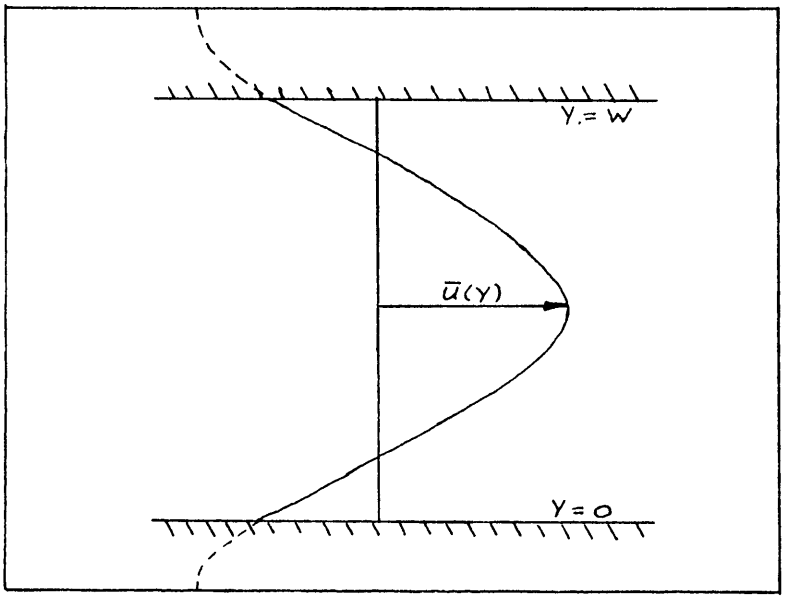

Fig. 4.1 Basic state velocity profile for R = 0.

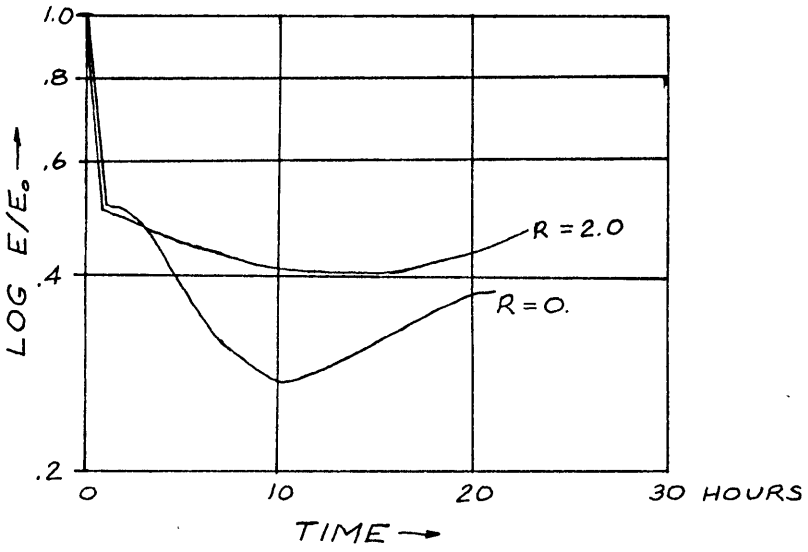

Fig. 4.2 Barotropic stability of the basic state.

V. THEORETICAL TREATMENT OF CENTRIFUGAL INSTABILITY

Having developed Eqs 4.3b, one might be tempted to proceed with an analysis of the stability of an arbitrary basic state $\overline{V}$. However, one might expect that the results would not be illuminating since the underlying assumption in this work is that the curvature of the flow has a direct bearing on its stability and Eqs 4.3b do not explicitly show how the curvature affects the flow.

To fix ideas, we consider a symmetric circular vortex in an incompressible homogeneous fluid. If we ignore the effect of gravity (i.e. no free surfaces or density discontinuities), the condition for stability of the vortex is that $R^{-3} \frac{\partial m^2}{\partial R} > 0$, where R is the radial coordinate and $m = RV = R(v + \Omega R)$ is the angular momentum, v the relative tangential velocity and Ω the angular rotation rate (for the proof and development of the above criterion see Charney (1973)). The criterion states that the square of the angular momentum must increase radially outward for stability.

Carrying out the differentiation, we obtain

$$2\left(\frac{v}{R} + \Omega\right)\left(2\Omega + \left(\frac{\partial v}{\partial R} + \frac{v}{R}\right)\right) > 0 \qquad (5.1)$$

The total relative vorticity of the flow $\frac{\partial v}{\partial R} + \frac{v}{R}$, consists of two parts, the vorticity due to the radial shear of the flow $\frac{\partial v}{\partial R}$ and the vorticity due to the curvature $\frac{v}{R}$. We then have the stability criterion in the form

$$(\Omega + \tfrac{v}{R})(2\Omega + \zeta) > 0 \qquad (5.2)$$

As we can see, the condition for stability depends on the sign of the absolute vorticity ($2\Omega + \zeta$) and the term $(\Omega + v/R)$.

Frequently one finds that the stability criterion is expressed in terms of the absolute vorticity alone, i.e.

$$2\Omega + \zeta > 0 \qquad (5.3)$$

In many problems of interest, $\Omega + v/R > 0$ and this condition is sufficient; however, it may happen that this term is negative (as in the case of strong anticyclonic flow), where the total vorticity may be negative and greater than -2Ω . In order to explore this possibility, we must recast Eqs 4.3b into a more suitable form.

In most problems of the stability of flows, the basic state is stationary and can be described rather simply in some coordinate system which reflects the geometry of the problem. In the more general case of stability of non-stationary flows, Eckart (1963) has shown that one can obtain

the Eulerian perturbation equations by a variational principle using generalized coordinates which are defined by the basic state rather than by the more common Lagrangian coordinates defined by the initial positions of the particles.

Since we already have the perturbation equations and since we have a steady-state basic state we need not go to the Lagrangian approach, but we need only to transform our coordinate system to the "natural coordinates" defined by our basic state. We may rewrite our perturbation Eqs 4.3b in vector notation:

$$\frac{\partial \mathbb{V}'}{\partial t} + R_o \overline{\mathbb{V}} \cdot \nabla \mathbb{V}' + R_o \mathbb{V}' \cdot \nabla \overline{\mathbb{V}} + f \hat{k} \times \mathbb{V}' = -\nabla h_2$$

$$\frac{\partial h_2}{\partial t} + R_o \overline{\mathbb{V}} \cdot \nabla h_2 + \frac{1}{\varepsilon(1+\gamma)} \nabla \cdot \mathbb{V}' = 0 \qquad (5.4)$$

Here the basic velocity $\overline{\mathbb{V}}$ defines a natural coordinate system as shown in Fig. 5.1. Let $V = |\overline{\mathbb{V}}|$, and let $\hat{t} = \overline{\mathbb{V}}/V = \frac{\overline{u}}{V}\hat{\imath} + \frac{\overline{v}}{V}\hat{\jmath}$ and $\hat{n} = -\frac{\overline{v}}{V}\hat{\imath} + \frac{\overline{u}}{V}\hat{\jmath}$ be the unit tangent and normal vectors at each point. We have now defined a right-handed coordinate system at each point in space such that $\hat{k} \times \hat{t} = \hat{n}$, except possibly at the points where $V = |\mathbb{V}|$ is zero. In the flows which we shall consider there are only a finite number of such points and for the most part we shall consider particle paths which do not have such singularities. The streamlines, Ψ = constant,

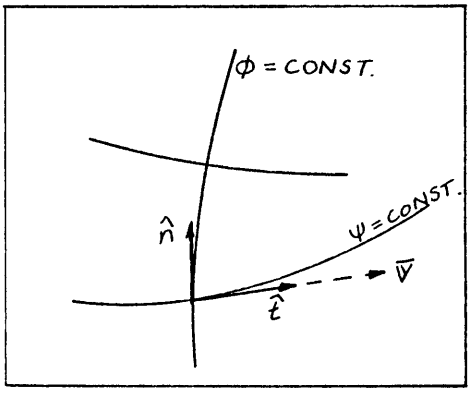

Fig. 5.1 Natural coordinates.

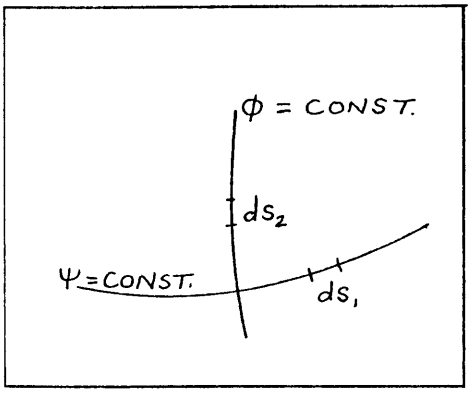

Fig. 5.2 Differential distances along coordinate curves.

of the basic state become one set of coordinate curves and the other, a set of orthogonal trajectories, ϕ = constant. Let ds_1 be the infinitesimal distance along curve ψ = constant and ds_2 the infinitesimal distance along the curve ϕ = constant (see Fig. 5.2). In terms of our $(\hat{t}, \hat{n})$ coordinates we can write

$$\begin{aligned} \bar{V} &= V\hat{t} \\ V' &= u\hat{t} + v\hat{n} \\ \nabla &= \frac{\partial}{\partial s_1}\hat{t} + \frac{\partial}{\partial s_2}\hat{n} \end{aligned} \tag{5.5}$$

We substitute Eqs 5.5 into Eqs 5.4 to obtain

$$\frac{\partial u}{\partial t} + R_o\left[V\frac{\partial u}{\partial s_1} + u\frac{\partial V}{\partial s_1} + v\left(\frac{\partial V}{\partial s_2} - \frac{V}{\rho_1}\right)\right] - fv = -\frac{\partial h_2}{\partial s_1}$$

$$\frac{\partial v}{\partial t} + R_o\left[V\frac{\partial v}{\partial s_1} - v\frac{V}{\rho_2} + \frac{2V}{\rho_1}u\right] + fu = -\frac{\partial h_2}{\partial s_2} \tag{5.6}$$

$$\frac{\partial h_2}{\partial t} + R_o V\frac{\partial h_2}{\partial s_1} + \frac{1}{\varepsilon(1+\delta)}\left[\frac{\partial u}{\partial s_1} + \frac{\partial v}{\partial s_2} - \frac{u}{\rho_2} - \frac{v}{\rho_1}\right] = 0$$

where we have made use of the Frenet formulas (see Hildebrand (1962)):

$$\frac{\partial \hat{t}}{\partial s_1} = \frac{\hat{n}}{\rho_1} \qquad \frac{\partial \hat{n}}{\partial s_1} = -\frac{\hat{t}}{\rho_1} \qquad \frac{\partial \hat{t}}{\partial s_2} = -\frac{\hat{n}}{\rho_2} \qquad \frac{\partial \hat{n}}{\partial s_2} = \frac{\hat{t}}{s_2}\ .$$

Here ρ_1 and ρ_2 denote the local radii of curvature of the curves ψ = constant and ϕ = constant, respectively.

As pictured in Fig. 5.1, both ς_1 and ς_2 are positive; ς_1 is positive for cyclonic curvature of ψ-curves and ς_2 is positive for anticyclonic curvature of ϕ-curves.

In natural coordinates the condition $\nabla \cdot \bar{V} = 0$ becomes

$$\frac{\partial V}{\partial s_1} - \frac{V}{\varsigma_2} = 0 \tag{5.7}$$

and $\bar{\zeta} = R_0 \left(\frac{V}{\varsigma_1} - \frac{\partial V}{\partial s_2} \right)$ is the relative vorticity of the basic state. We then rewrite Eqs 5.5 in the form

$$\left(\frac{\partial}{\partial t} + R_0 V \frac{\partial}{\partial s_1} \right) u + R_0 \frac{V}{\varsigma_2} u - (f + \bar{\zeta}) v = - \frac{\partial h}{\partial s_1}$$

$$\left(\frac{\partial}{\partial t} + R_0 V \frac{\partial}{\partial s_1} \right) v - R_0 \frac{V}{\varsigma_2} v + \left(f + \frac{2 R_0 V}{\varsigma_1} \right) u = - \frac{\partial h}{\partial s_2} \tag{5.8}$$

$$\left(\frac{\partial}{\partial t} + R_0 V \frac{\partial}{\partial s_1} \right) h + \frac{1}{\varepsilon (1+\delta)} \left[\frac{\partial u}{\partial s_1} + \frac{\partial v}{\partial s_2} - \frac{u}{\varsigma_2} - \frac{v}{\varsigma_1} \right] = 0$$

If we set $\bar{V} = \bar{V}(r)$, $ds_1 = r d\theta$, $ds_2 = -dr$, $\varsigma_2 = \infty$, then the basic state becomes the classical circular vortex, and Eqs 5.8 reduce to the usual perturbation equations for a circular vortex.

The basic assumption in perturbation expansions is that the perturbation quantities are much smaller than those of the basic state, i.e. $u << V$. This implies that the fluid particles have trajectories which almost coincide with those of the basic state. We may choose $u(t=0)$ so small

that

$$\int_0^T u\, dt \ll \int_0^T V\, dt$$

over any time T we wish to consider. We therefore express the substantial derivative of any variable as

$$\frac{d}{dt} = \frac{\partial}{\partial t} + R_0 V \frac{\partial}{\partial s_1} \tag{5.9}$$

so that Eqs 5.8 may be interpreted as the Langrangian perturbation equations for a particle. This connection between the Eulerian and Lagrangian equations was demonstrated by Eckart (1963), starting from the Lagrangian point of view and identifying the generalized coordinates not with the initial positions of the particles but with their paths as defined by the basic state.

Eqs 5.8 may now be written

$$\begin{aligned} &\frac{du}{dt} + \eta u - (f + \bar{\zeta}) v = -\frac{\partial h}{\partial s_1} \\ &\frac{dv}{dt} - \eta v + (f + c) u = -\frac{\partial h}{\partial s_2} \\ &\frac{dh}{dt} + \delta \left\{ \frac{\partial u}{\partial s_1} + \frac{\partial v}{\partial s_2} - \frac{u}{\rho_2} - \frac{v}{\rho_1} \right\} = 0 \end{aligned} \tag{5.11}$$

where

$$\eta := \frac{R_0 V}{\rho_2}, \quad c = \frac{2 R_0 V}{\rho_1}, \quad \delta = \frac{1}{\varepsilon(1+\gamma)}.$$

(We remark that f = 1 non-dimensionally, but we retain the symbol as a reminder of where the term came from.)

We shall now do a "local" stability analysis to obtain some insight into the nature of centrifugal instability. We assume that, although the coefficients are variables, their variations are slow in comparison with the variations in u, v, and h. With this assumption, we let $(u, v, h) \sim (u_0, v_0, h_0) e^{i(k s_1 + l s_2 - \omega t)}$ where $k, l >> 1/\varsigma_1 , 1/\varsigma_2$.

Eqs 5.11 have a non-trivial solution if

$$\begin{vmatrix} (-i\omega + \eta) & -(f+\bar{\varsigma}) & ik \\ (f+c) & (-i\omega - \eta) & il \\ i\delta k & i\delta l & -i\omega \end{vmatrix} = 0 \qquad (5.12)$$

We note that in terms of the Eulerian equations, ω is merely the Doppler shifter frequency, i.e. $\omega = \tilde{\omega} - kR_0V$. From Eqn 5.12 we get the characteristic equation for ω :

$$-i\omega \{ \omega_c^2 - \eta^2 - \omega^2 + \delta(k^2+l^2) \} + \delta \{ \eta(l^2-k^2) + lk(\bar{\varsigma} - c) \} = 0 \qquad (5.13)$$

where $\omega_c^2 \equiv (f+\bar{\varsigma})(f+c)$. We shall now examine an interesting special case.

The Axisymmetric Circular Vortex

In this case ς_1 is identified with the usual radial coordinate r. $\varsigma_2 \to \infty$ and therefore $\eta \to 0$. If we still permit perturbations in the r and θ directions,

Eqn 5.13 becomes

$$\omega \{ \omega_c^2 - \omega^2 + \delta(k^2+l^2) \} + i \delta l k (\bar{s} - c) = 0 \qquad (5.14)$$

The term in braces yields the same criterion as one would obtain by more exact treatments of the circular vortex (see Eqn 5.2) with the additional stabilizing term $\delta(k^2+l^2)$. The additional term $i\delta l k(\bar{s}-c)$ is most likely due to the nature of our analysis and probably has no physical significance. It does not appear if we limit the perturbation to be axisymmetric.

We shall now look at a more exact treatment of Eqs 5.11, making the simplifying assumption that there is little or no dependence on s_2. We make this assumption based on the numerical results presented in the next chapter, where one can see that the perturbation is essentially oriented so that the wave crest are perpendicular to the streamlines, at least in the region of strongest instability. This allows us to assume that the perturbation is a function only of s_1 and t. This is contrary to the usual analysis of centrifugal instability where $\frac{\partial}{\partial s_1}$ is assumed to be zero. Since the coefficients of Eqs 5.11 are independent of t, we assume

$$(u, v, h) = e^{i\omega t} (u(s), v(s), h(s)) \qquad (5.19)$$

where $s \equiv s_1$. If $\frac{\partial}{\partial s_2} \equiv 0$ and putting 5.19 into 5.11 we obtain

$$\begin{aligned} (-i\omega + \eta)u \; - \; (f + \bar{\varepsilon})v \; + \; \frac{\partial h}{\partial s} &= 0 \\ (f + c)u \; - \; (i\omega + \eta)v \; &= 0 \\ \delta\left(\frac{\partial u}{\partial s} - \frac{u}{\rho_2}\right) \; - \delta\frac{v}{\rho_1} \; - i\omega h &= 0 \end{aligned} \tag{5.20}$$

Eliminating v(s) and h(s) from Eqs 5.20, we obtain an equation for u(s):

$$\begin{aligned} &\frac{\partial^2 u}{\partial s^2} \; - \left(\frac{1}{\rho_2} \; + \; \frac{f + c}{\rho_1(\eta + i\omega)}\right)\frac{\partial u}{\partial s} \\ &\quad + \left\{\frac{i\omega}{\delta(\eta + i\omega)}(\omega^2 + \eta^2 - \omega_c^2) - \frac{\partial}{\partial s}\left(\frac{1}{\rho_2} + \frac{f + c}{\rho_1(\eta + i\omega)}\right)\right\} u = 0 \end{aligned} \tag{5.21}$$

Making the definitions

$$\begin{aligned} \alpha(s) &= -\left(\frac{1}{\rho_2} \; + \; \frac{f + c}{\rho_1(\eta + i\omega)}\right) \\ \beta(s) &= \left\{\frac{i\omega}{\delta(\eta + i\omega)}(\omega^2 + \eta^2 - \omega_c^2) \; + \; \frac{\partial \alpha}{\partial s}\right\} \end{aligned} \tag{5.22}$$

where ω_c^2 is as defined in Eqn 5.13, we rewrite Eqn 5.22 as

$$\frac{\partial^2 u}{\partial s^2} \; + \alpha(s)\frac{\partial u}{\partial s} \; + \beta(s)u = 0 \; . \tag{5.23}$$

If we make the transformation

$$u(s) = p(s)\mu(s) \tag{5.24a}$$

where

$$p(s) = \exp\left[-\tfrac{1}{2}\int_0^s \alpha(\lambda)\, d\lambda \right. \tag{5.24b}$$

we obtain an equation for $\mu(s)$:

$$\frac{\partial^2 \mu}{\partial s^2} + \left[\beta(s) - \frac{1}{2}\frac{\partial \alpha}{\partial s} - \frac{1}{4}\alpha^2\right]\mu = 0 \tag{5.25}$$

We rewrite 5.25 as

$$\delta \frac{\partial^2 \mu}{\partial s^2} + \left\{ \frac{i\omega}{\eta + i\omega}(\omega^2 + \eta^2 - \omega_c^2) + \delta\left(\frac{1}{2}\frac{\partial \alpha}{\partial s} - \frac{1}{4}\alpha^2\right)\right\}\mu = 0 \tag{5.26}$$

One should note several things about Eqn 5.26. First, since we have the small parameter δ in the equation, we might be tempted to do a perturbation expansion. However, δ multiplies the highest derivative, thereby making this a singular perturbation problem. We can get around this problem by transforming to stretched coordinates $s = \delta^{1/2}\sigma$. This leads to a second order equation with complex coefficients. Since the particles travel on closed streamlines, Eqn 5.26 has periodic coefficients. By imposing the condition that the solutions $\mu(s)$ also be periodic in s, we have an eigenvalue problem where ω is the eigenvalue to be determined. The general theory of such equations is known as Floquet theory (see Whitaker and Watson (1927), Ince (1926) or Lefshetz (1948)).

In general, the solutions to such equations need not be

periodic and in addition may have exponentially growing solutions. We shall merely note that the determination of admissable solutions is not a trivial matter.

VI. RESULTS OF NUMERICAL EXPERIMENTS

Having developed the model with which one might study centrifugal instability, we shall now discuss the results derived therefrom and try to relate these results to the theory outlined in Chapter V. The model Eqs 4.3b were integrated numerically using standard finite difference procedures, which are detailed in Appendix B. The computations were done on a channel of cross section 4000 km and length 8000 km. The grid size was 50 km in both the x and y directions and a time step of 5 minutes was chosen to be compatible with the Courant-Friedrichs-Lewy stability criterion at all values of the paramters $\mathcal{E}$ and R_0. We note that changing the parameter R changes the shape of the streamlines (compare Figs. 6.1 - 6.3), the parameter R_0 changes the ratio of $\bar{\zeta}$ to f, and the parameter $\mathcal{E}$ influences the stabilizing effects of the divergence of the perturbation. (Also note that decreasing the value of $\mathcal{E}$ is equivalent to increasing the phase speed of the gravity waves (see Eqn 2.2).)

We shall now examine the streamlines of the basic state, which are given by Eqn 3.7. Figs. 6.1, 6.2, and 6.3 show the streamline pattern for values of the parameter R = 2.0, 1.0, 0.5 respectively. We see that as R decreases, the closed circulations become flatter. This has several effects. The first is to decrease the curvature of the closed

circulations in the regions labeled r_2. We also note that regions r_1 are regions of strong confluence and difluence of the streamlines which, as discussed in Chapter V, may have an effect on the stability of the flow. In this connection, we have sketched several lines in Fig. 6.1 which are the cross-streamline coordinates in our natural coordinate system. We see that these lines have larger values of curvature in regions r_1. This effect is quite pronounced in Fig. 6.3.

In all cases, the constant A in Eqn 3.7 is chosen so that $|\nabla^2\psi|_{max} \leq 1$. This implies that the absolute vorticity, $1 + R_o\zeta$, is negative only if R_o is large enough. Thus, we can change the shape of the streamlines by adjusting the parameter R and we can independently adjust the absolute vorticity maximum by changing R_o.

We shall now consider the detailed nature of one experiment so that we have a picture of what is occurring in an Eulerian framework. In Figs. 6.4 - 6.14, we have contoured the interface perturbation height for the parameters R_0 = 1.0, R = 1.0, $\mathcal{E}$ = 50. The corresponding streamlines are given in Fig. 6.2. The figures show the h field at hourly intervals from 10 hours to 20 hours of model time. During first 10 hours of the run, the model was organizing the perturbation and there is considerable randomness due to the initial random perturbation of the v velocity field. The contours are given as multiples of σ, the standard deviation of h about the mean, which is always zero. This allows us to focus

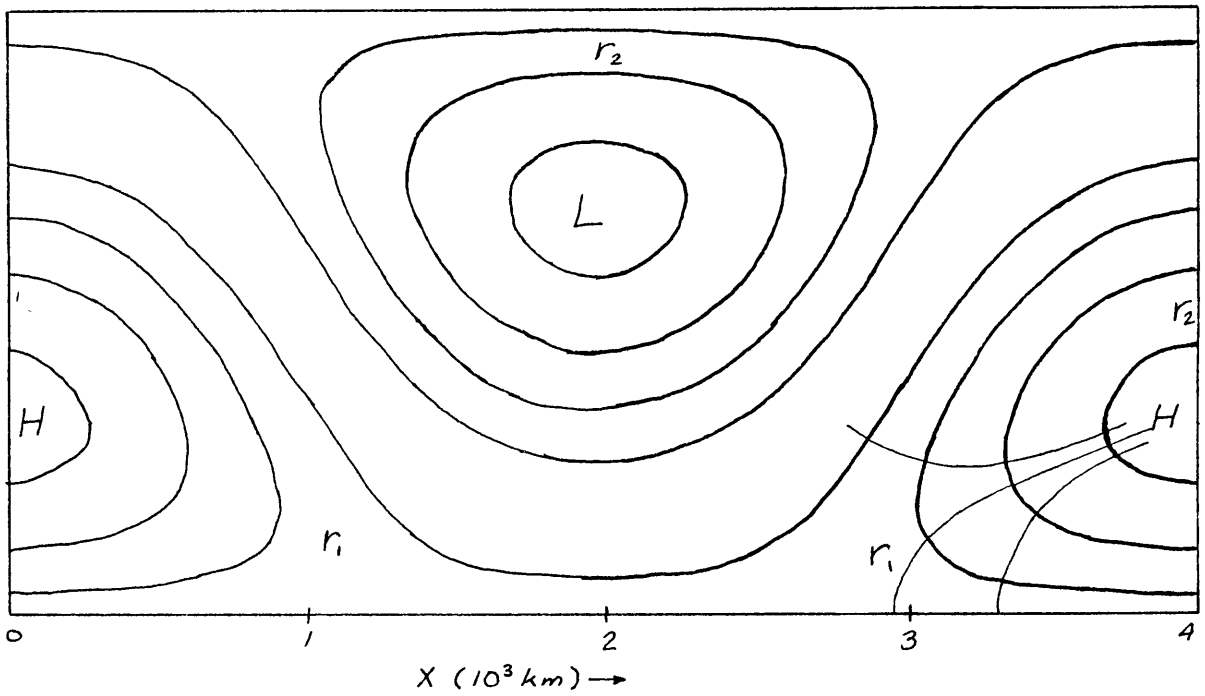

Fig. 6.1 Basic state stream function (R = 2.0). Orientation is that of Fig. 1.1.

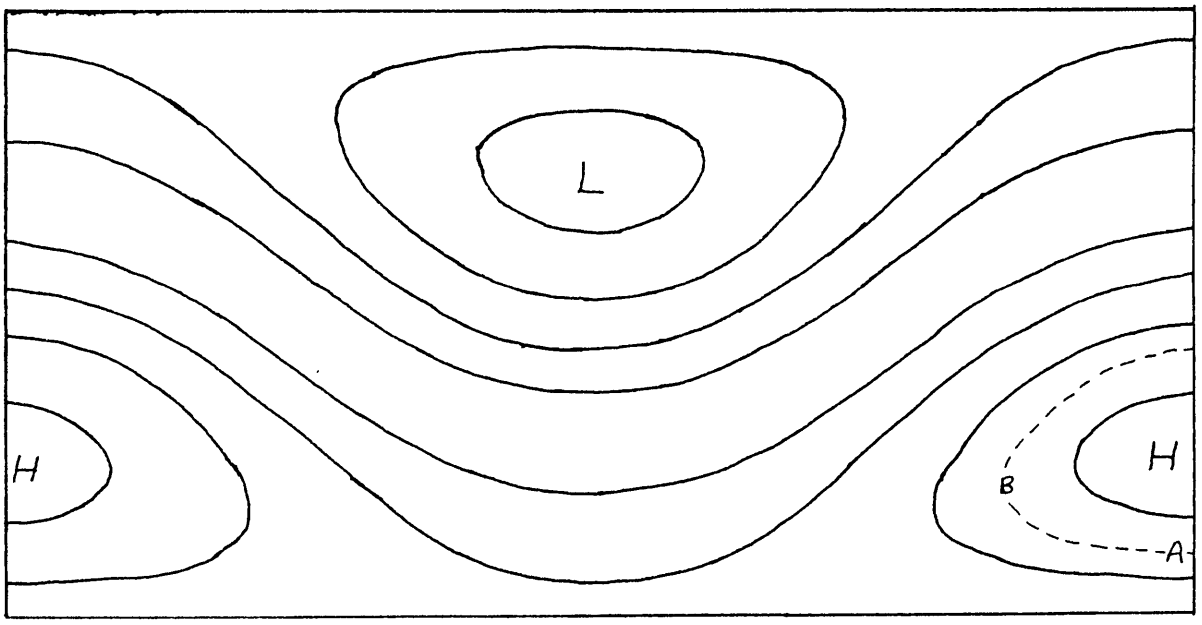

Fig. 6.2 Basic state stream function (R = 1.0).

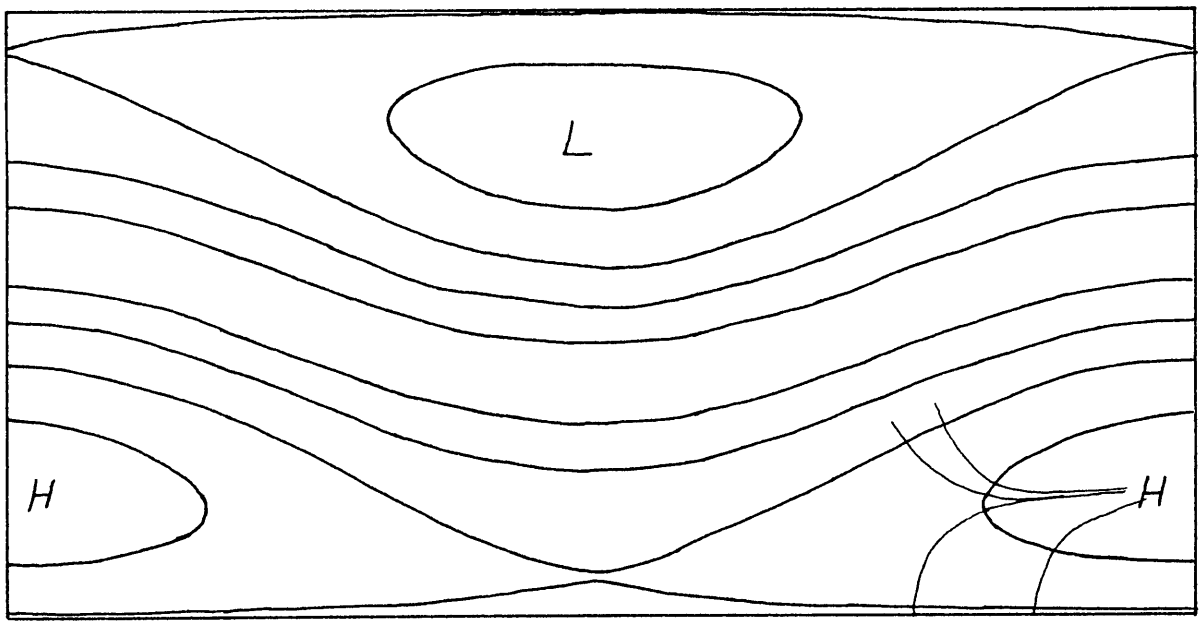

Fig. 6.3 Basic state stream function (R = 0.5).

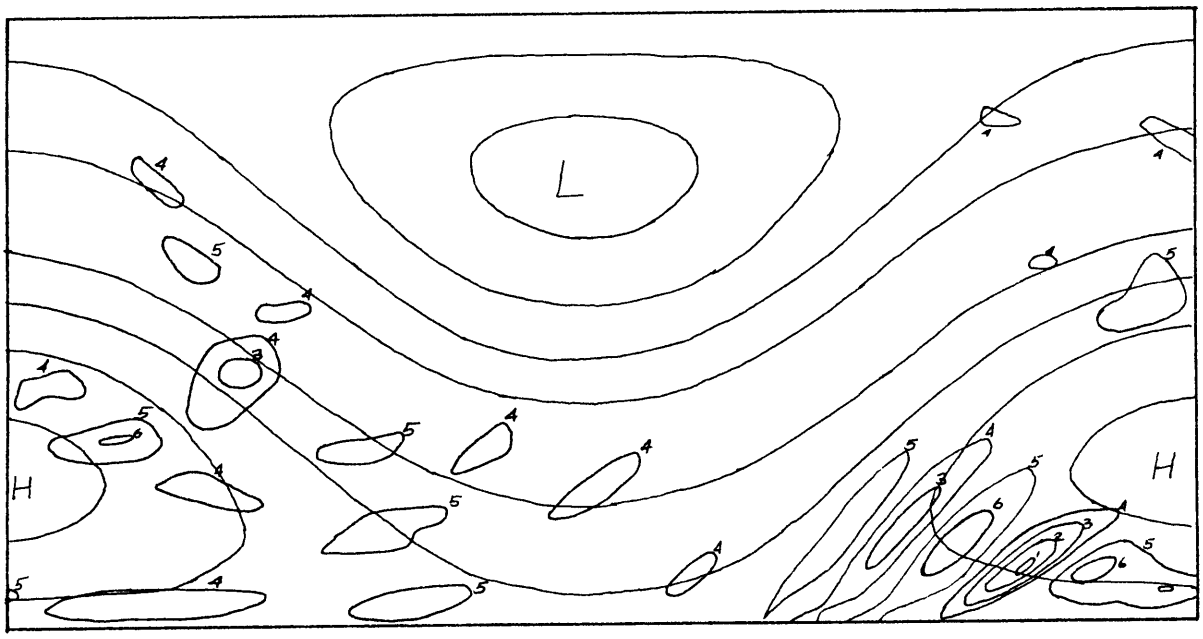

Fig. 6.4 Contours of σ(h) (see text) for time t = 10 hours. Contour values are:

1 - -6σ	5 - 1.5σ
2 - -4.5σ	6 - 3σ
3 - -3σ	7 - 4.5σ
4 - -1.5σ	8 - 6σ

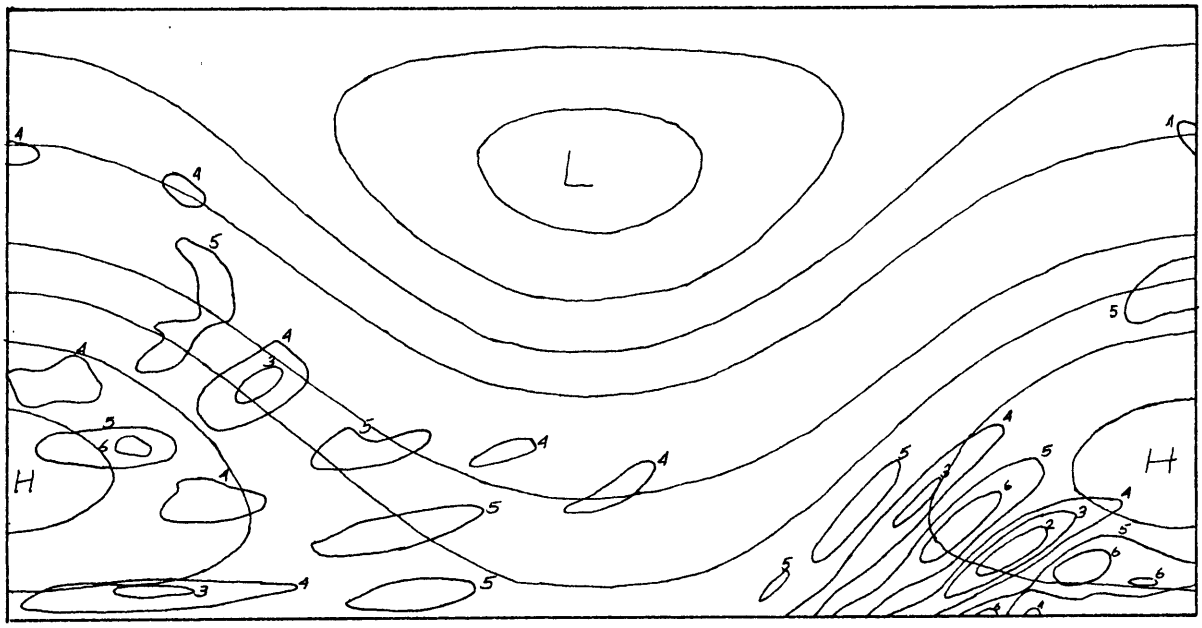

Fig. 6.5 Same as Fig. 6.4, t = 11 hours.

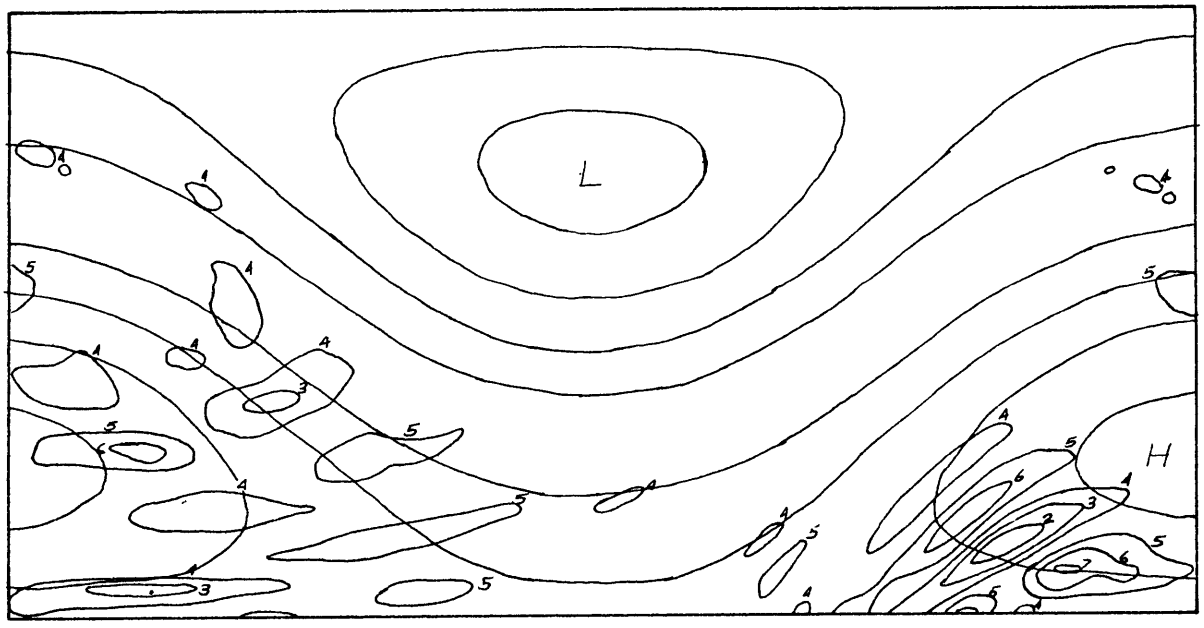

Fig. 6.6 Same as Fig. 6.4, t = 12 hours.

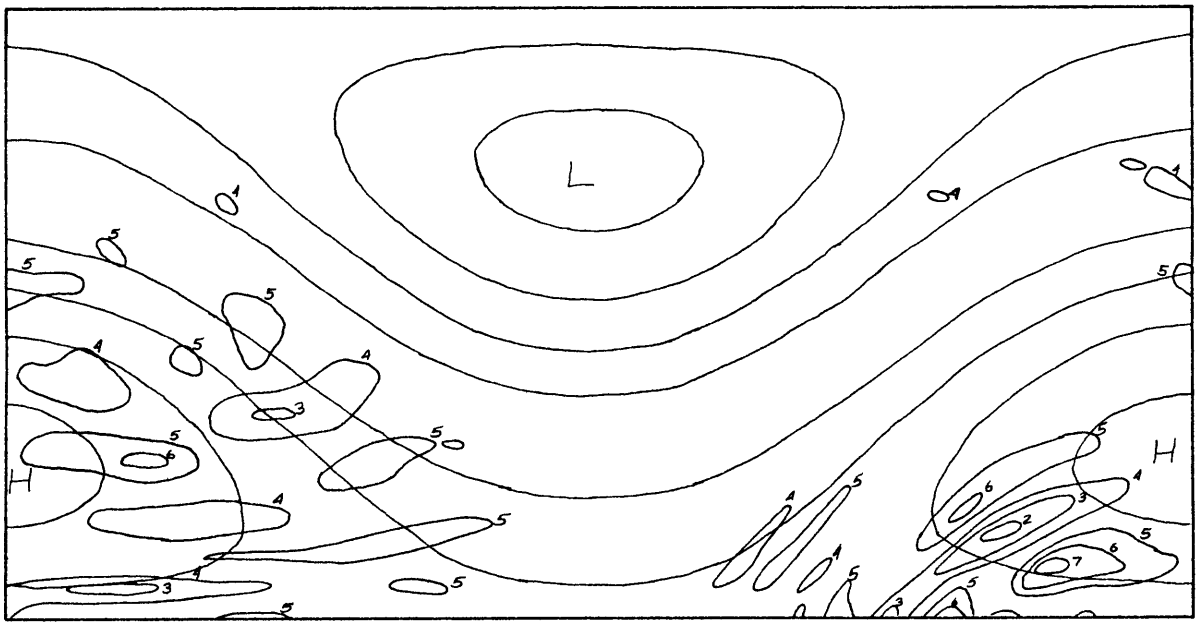

Fig. 6.7 Same as Fig. 6.4, t = 13 hours.

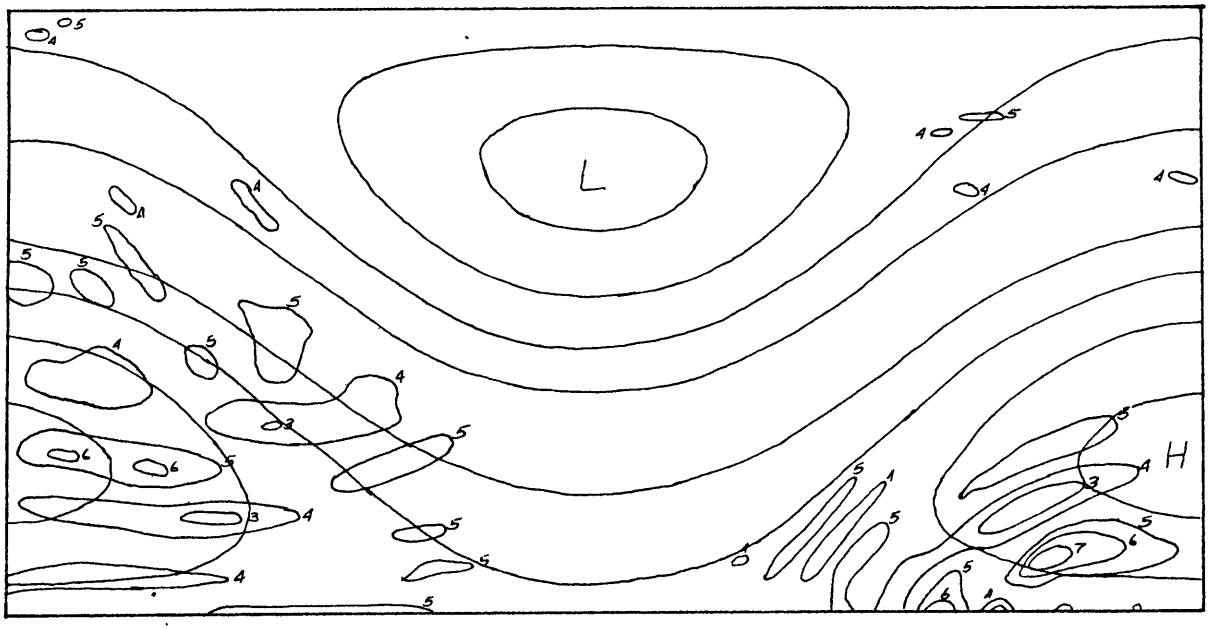

Fig. 6.8 Same as Fig. 6.4, t = 14 hours.

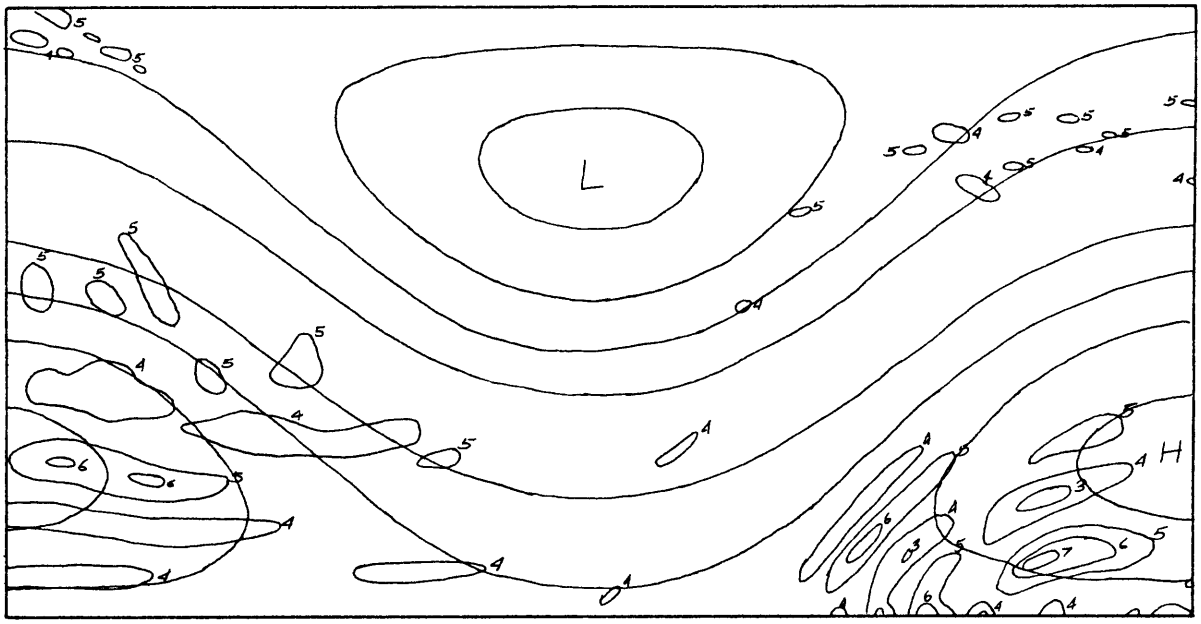

Fig. 6.9 Same as Fig. 6.4, t = 15 hours.

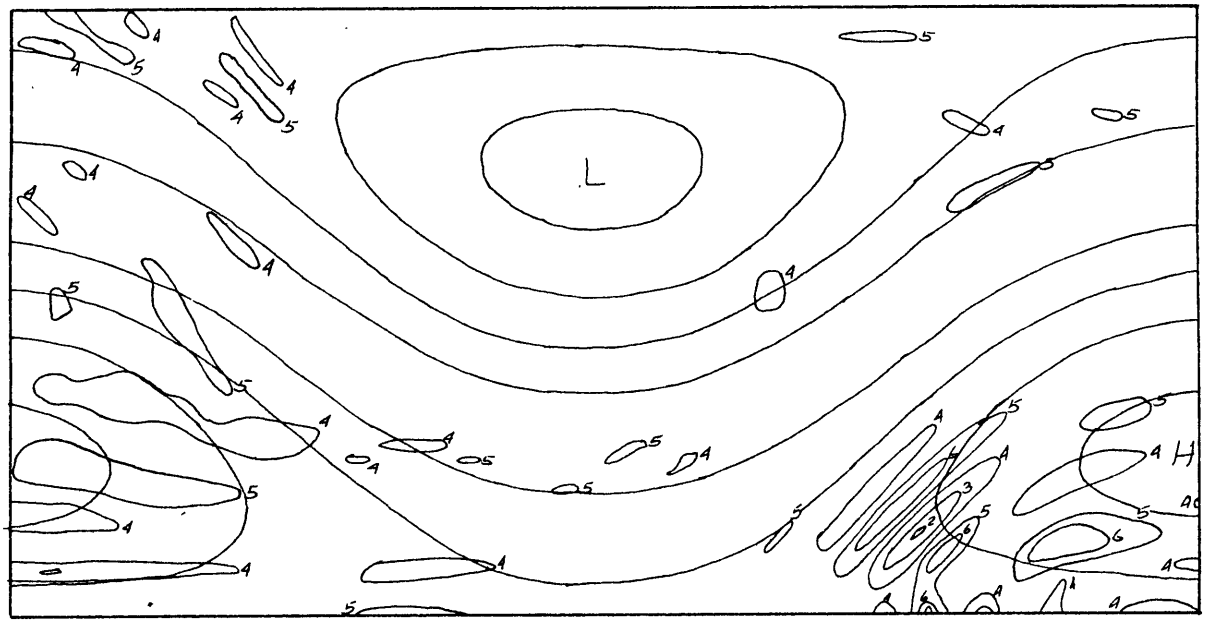

Fig. 6.10 Same as Fig. 6.4, t = 16 hours.

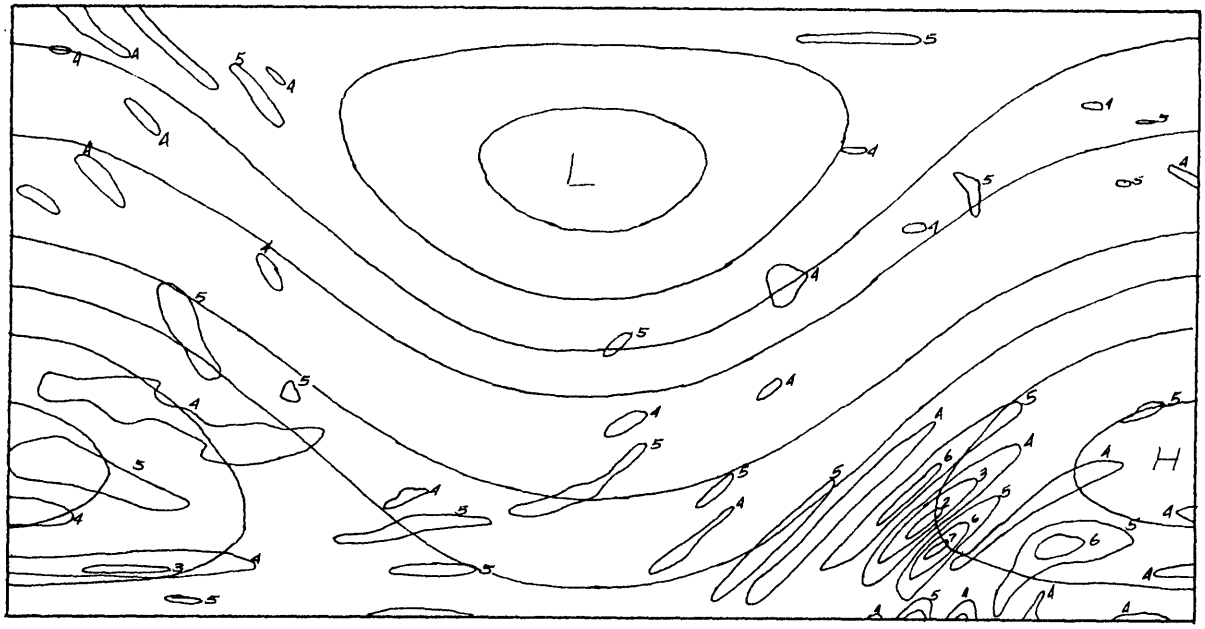

Fig. 6.11 Same as Fig. 6.4, t = 17 hours.

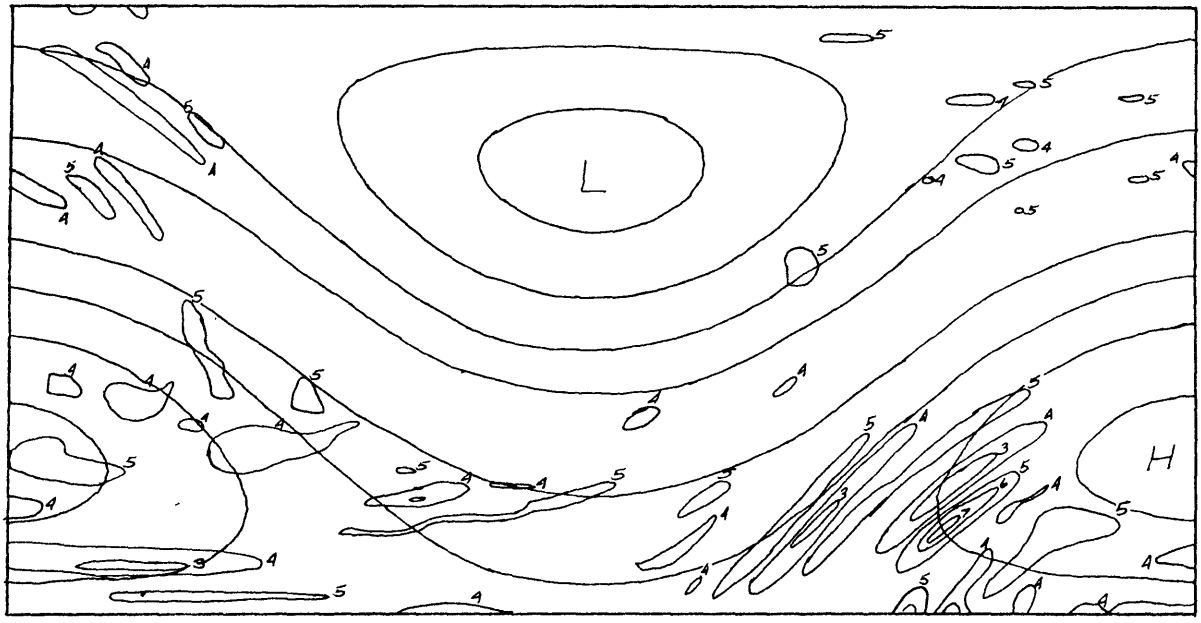

Fig. 6.12 Same as Fig. 6.4, t = 18 hours.

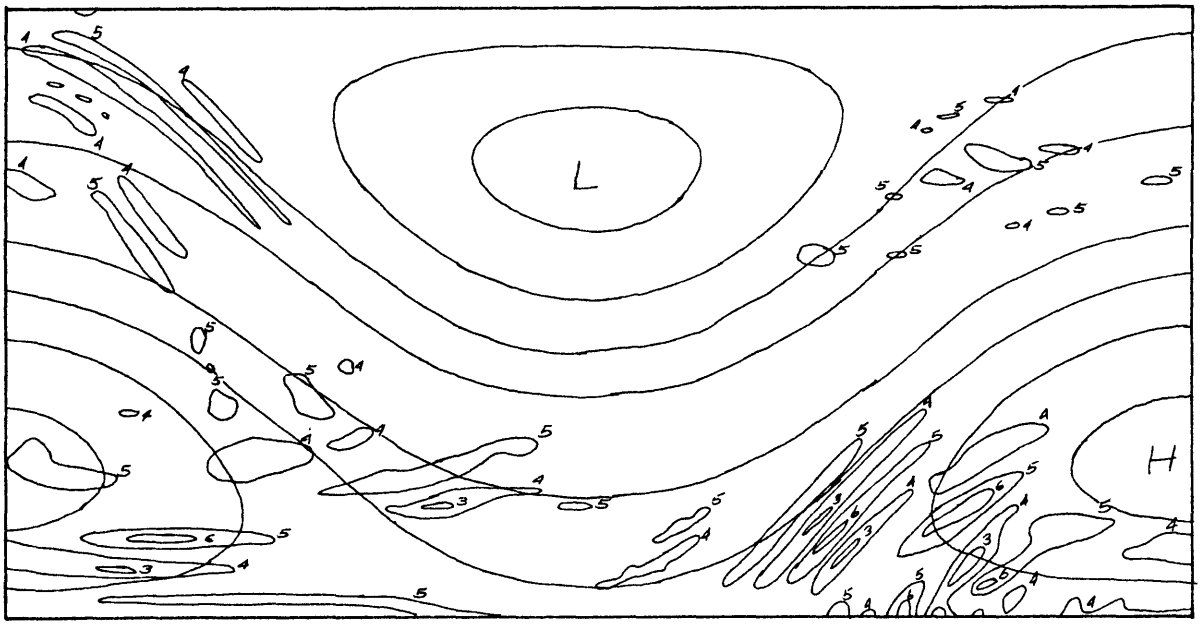

Fig. 6.13 Same as Fig. 6.4, t = 19 hours.

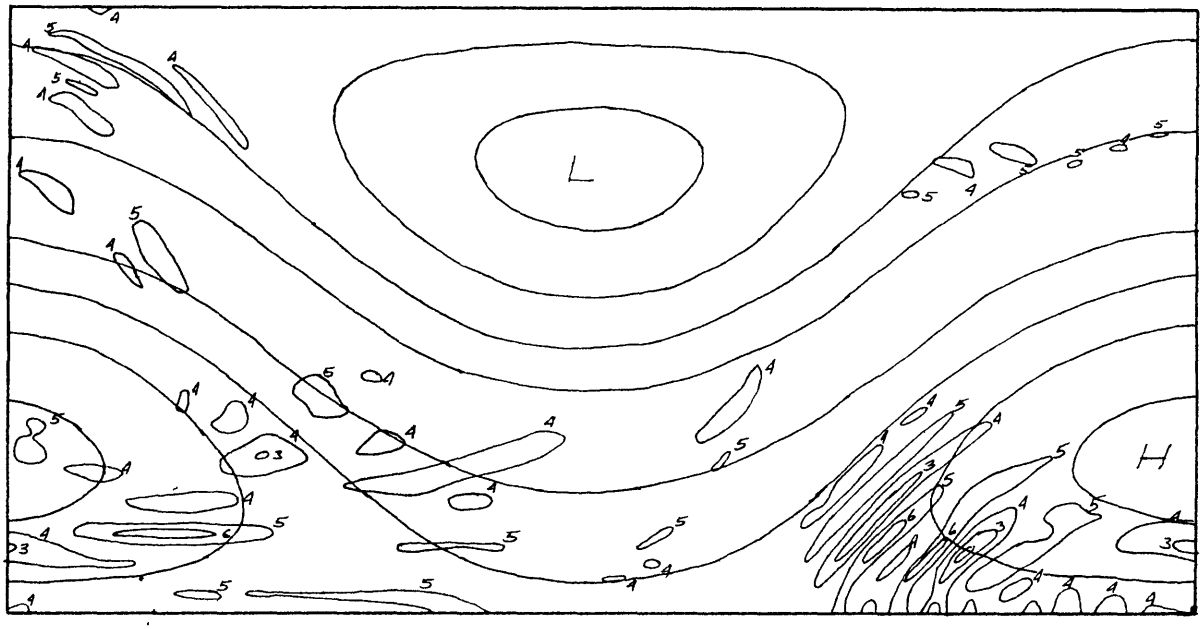

Fig. 6.14 Same as Fig. 6.4, t = 20 hours.

on the significant features and to eliminate most of the background noise from the picture.

The most important feature, in terms of structure and magnitude, occurs in the lower right hand corner. This is a region of strong anticyclonic curvature and streamline confluence. The wave crests are oriented more or less perpendicular to the streamlines; this is the basis for our assumption in Chapter V. The line along the wave crests is oriented with the region which has a minimum value for ω_c^2 (Eqn 5.2). The tilt of the wave crests may also be due to the shear in the basic state. The velocity near the wall is larger than near the center of the high (note that the wall is a streamline) and therefore one might expect this configuration.

The wavelength of this disturbance is ~ 800 km at 10 hours. By 15 hours, this feature has diminished in extent and magnitude and has been advected away from its source region by the mean flow. At the same time, starting at 14 hours, we see the development of a new wave packet which grows and then dissipates by 19 hours. The wave-length of this second feature is ~ 350 km. From this point on in time one sees continual growth and decay of features such as this, with a scale of ~ 350 km. As the integration is carried out further in time the waves have a more fractured, small scale structure, which may be due to the limitation of the grid in resolving the steep height gradients.

Other features during this time frame are less well structured and of generally smaller magnitude. In the lower left corner, along the bottom boundary is a feature which persists for some time. Its orientation is along the streamlines rather than across them. Its significance is that disturbances generated here tend to propagate into the region of major activity.

At this point, we should consider a physical explanation for these phenomena. One simple explanation which comes to mind is that on the right, between points A and B in Fig. 6.2, fluid particles are slowing down, reaching a maximum speed at the line of curvature, and therefore any conserved quantity, such as potential vorticity, would pile up in this region. The feature near the wall at the lower left might be explained by a similar argument. However, we have exactly the same situation around the low, but there is no evidence of such strong wave generation. We must therefore conclude that the flow being anticyclonic is of major importance in determining this instability.

Another aspect of the stability problem is the growth of the total perturbation energy in time. The perturbation energy of the system is

$$E = u^2 + v^2 + \varepsilon(1+\gamma)h^2 \qquad (6.1)$$

(In writing the finite difference analogue of Eqs 4.3b, it is somewhat more convenient to use the nondimensional variable $\hbar = \varepsilon R_o(1+\gamma)h$. Thus the energy is calculated as $E = u^2 + v^2 + (\varepsilon R_o^2(1+\gamma))^{-1}\hbar^2$. See Appendix B.)

In Fig. 6.15, we have plotted total energy E divided by E(t = 0) versus time. R_0 and ε are fixed and R varies from .5 to 2.0, as indicated in the figure. The first thing we note is that in the first 40 hours, the growth rates are fastest for larger values of R. For R = 2.0 we get a doubling time of 36 hours while for R = 0.5 we get 67 hours. The second feature of these curves is that for intermediate values of R (1.0-1.5), the growth in E very nearly levels off, as if a steady state had been reached. It is clear from these results that the dependence on R is quite complex and we have no simple explanation of these results.

In Fig. 6.16 we see a much simpler aspect of the problem. For fixed R = 1.0 and ε = 200, as R_0 increases we get an increase in the growth rate of E. This is more easily explained since our stability criterion is

$$\omega_c^2 = (1 + R_o\bar{\zeta})\left(1 + \frac{2R_oV}{\rho_1}\right) > 0 \qquad (6.2)$$

In Figs. 6.18 - 6.22, we have contoured values of ω_c^2 for various values of R_0, keeping R = 1.0. In general, we see that the regions of strongest anticyclonic curvature have negative values of ω_c^2 . There is a slight discrepancy

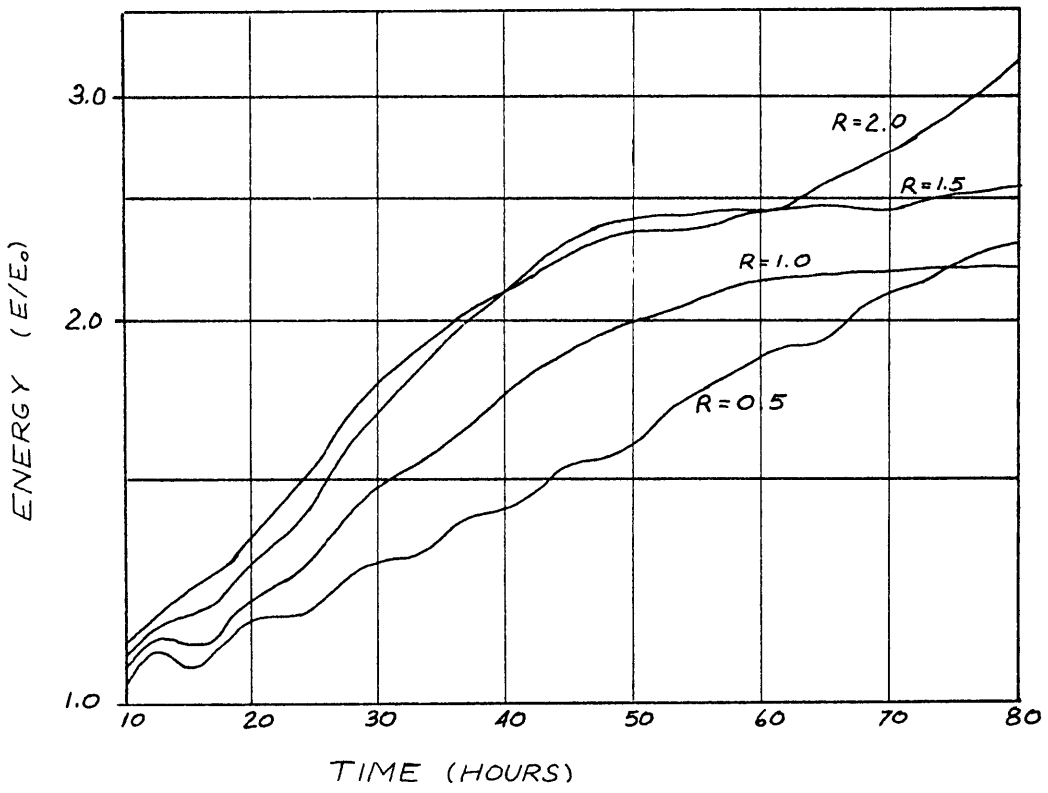

Fig. 6.15 Total perturbation energy versus time for $\mathcal{E} = 200$, $R_0 = 1.0$ for various values of R.

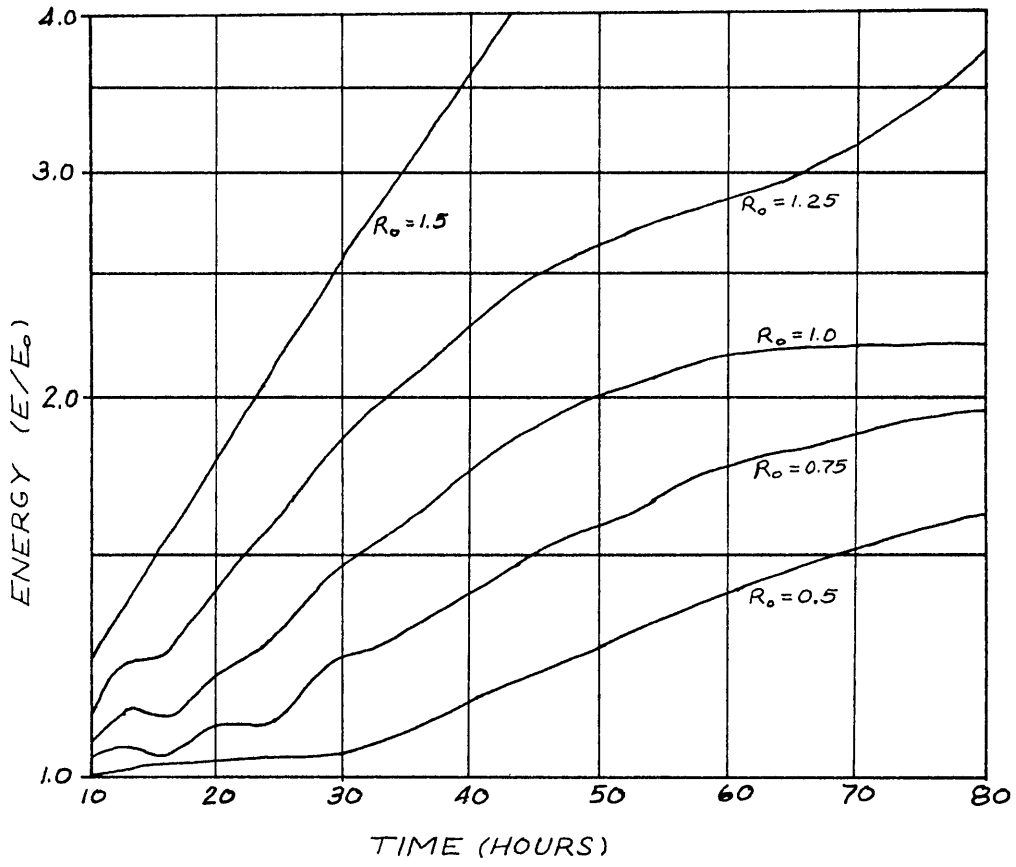

Fig. 6.16 Same as Fig. 6.15 for $\mathcal{E}$ = 200, R = 1.0 for various values of R_0.

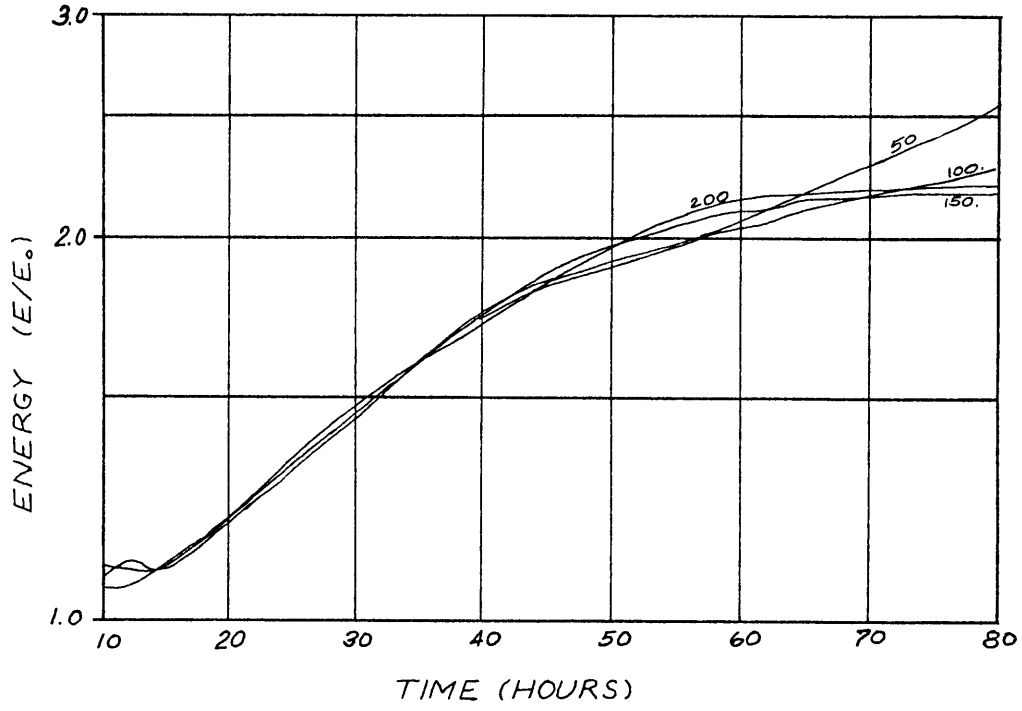

Fig. 6.17 Same as Fig. 6.15 for $R_0 = 1.0$, $R = 1.0$ for various values of $\mathcal{E}$.

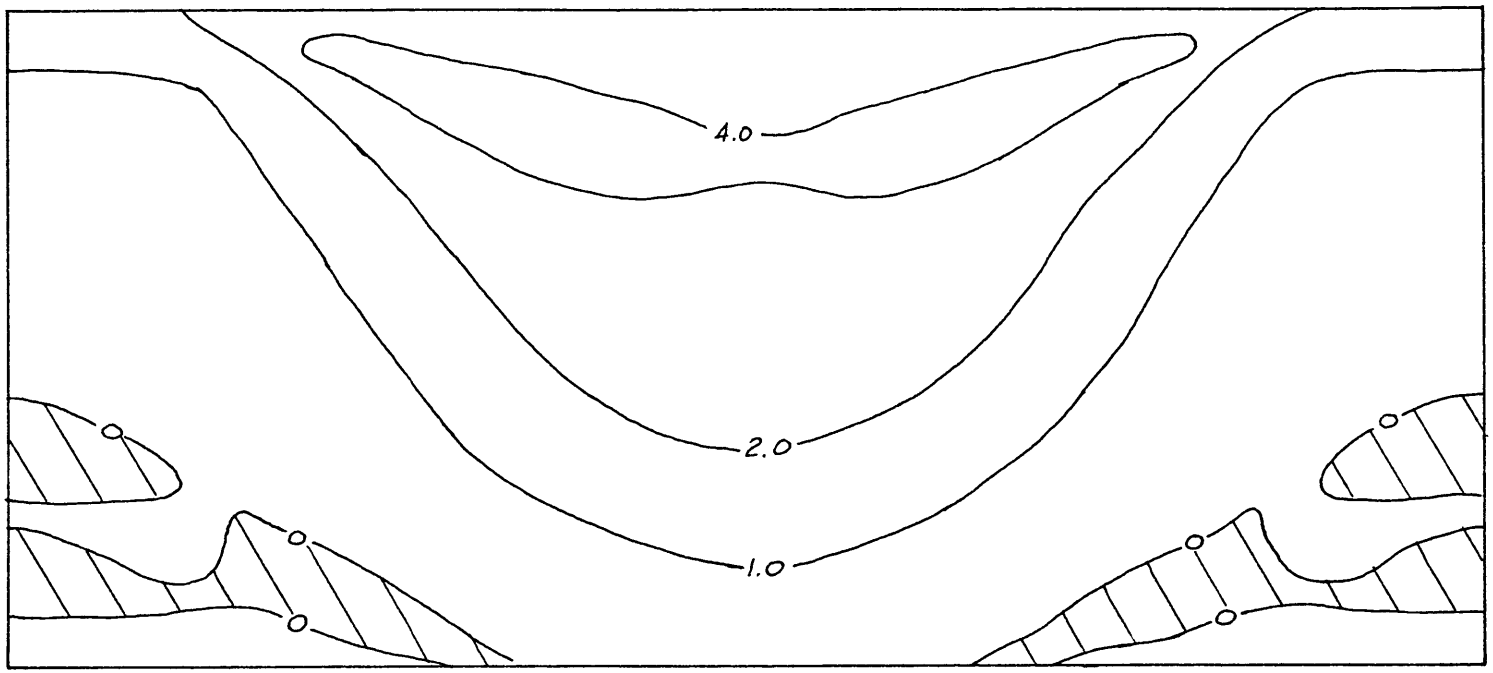

Fig. 6.18 Contours of the stability parameter ω_c^2 (see text). Hatched areas have values of $\omega_c^2 < 0$. R = 1.0, R_0 = 1.5. Min ω_c^2 = -0.20.

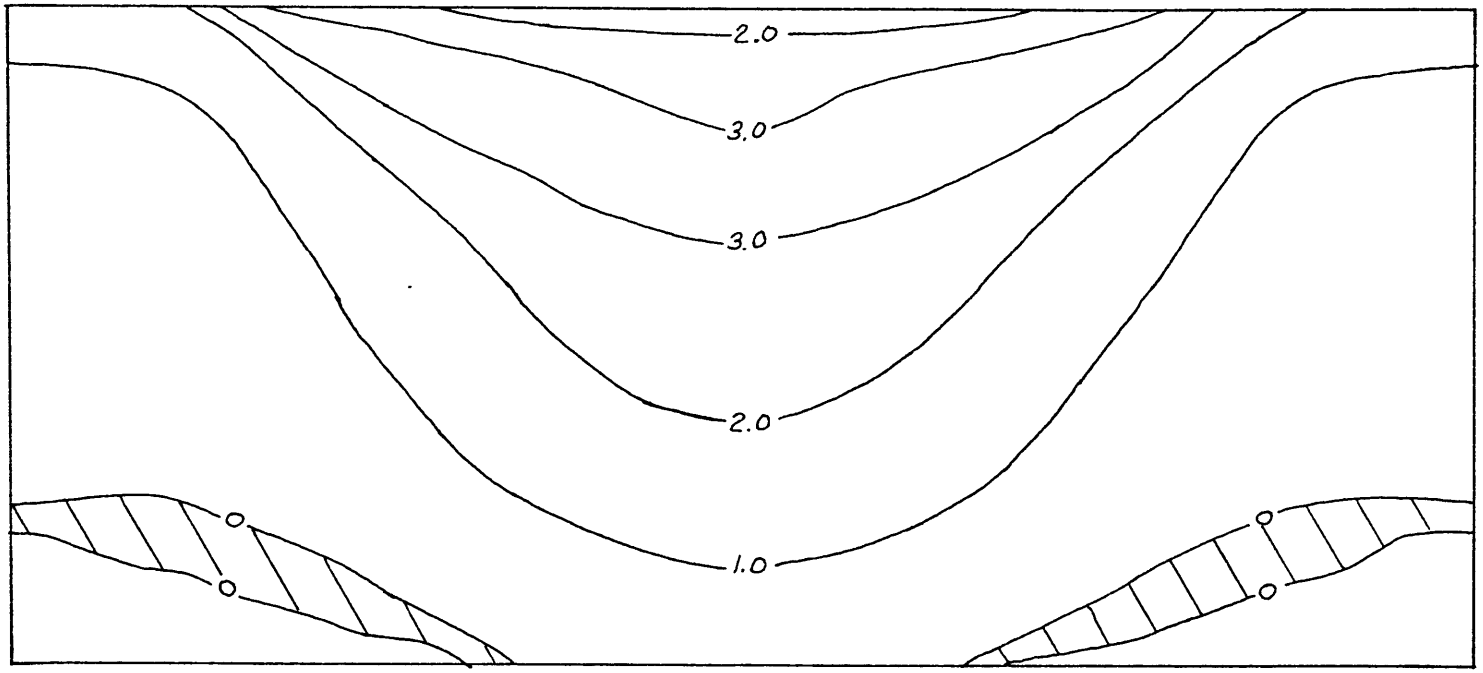

Fig. 6.19 Same as Fig. 6.18. $R_0 = 1.25$, Min $\omega_c^2 = -0.16$.

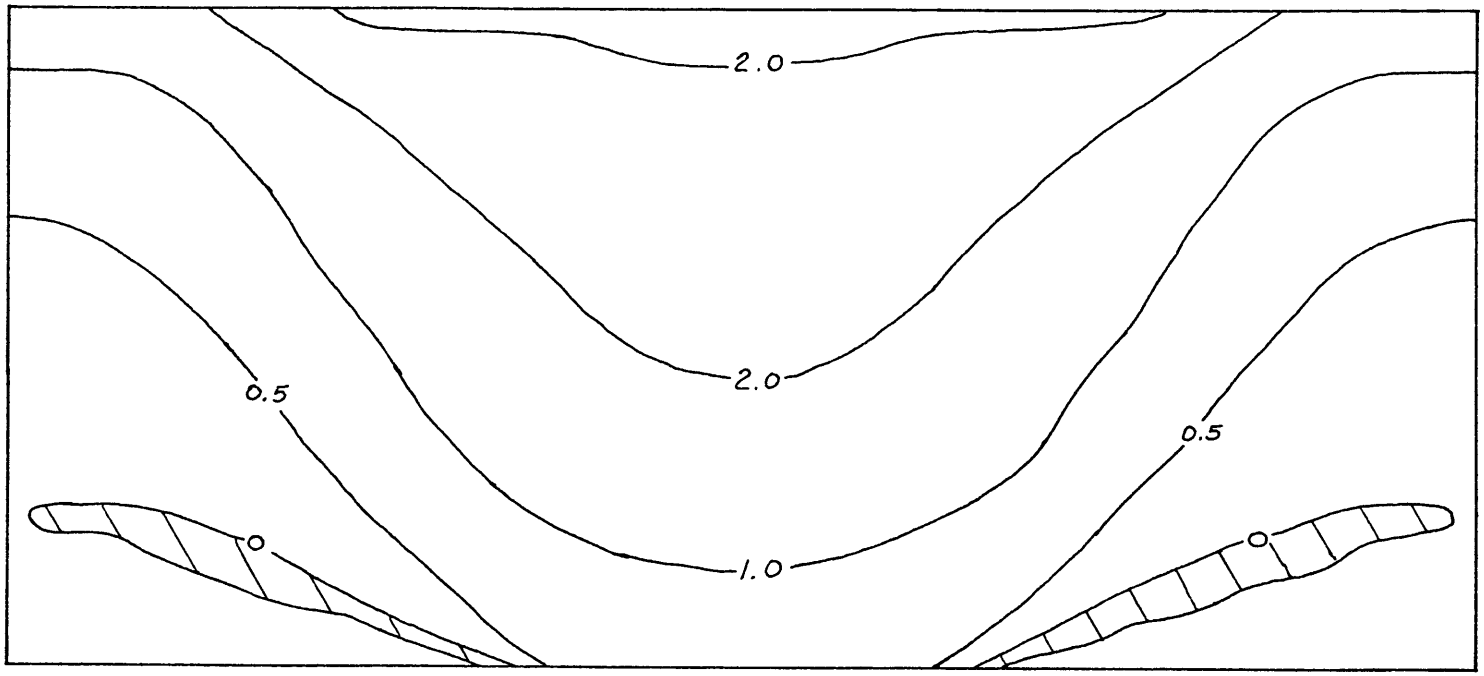

Fig. 6.20 Same as Fig. 6.18. R_0 = 1.0, Min ω_c^2 = -0.09.

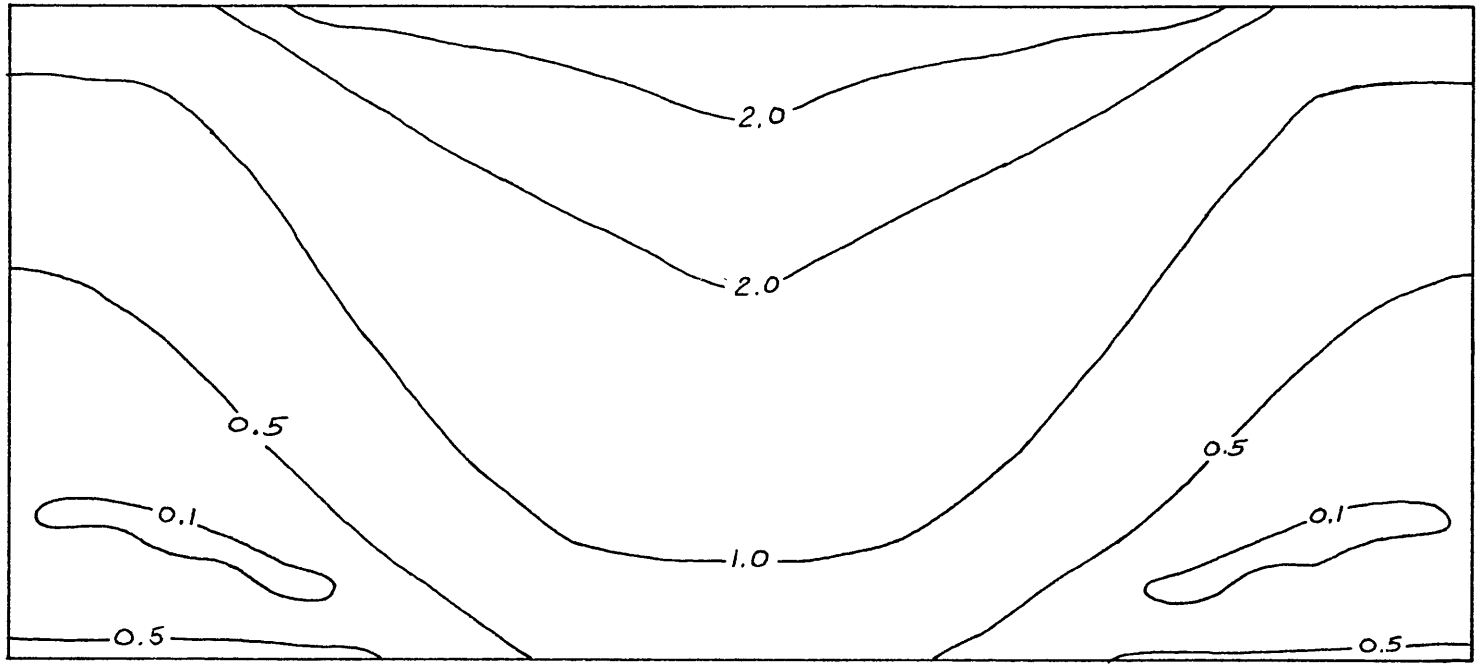

Fig. 6.21 Same as Fig. 6.18. R_0 = 0.75, Min ω_c^2 = 0.03.

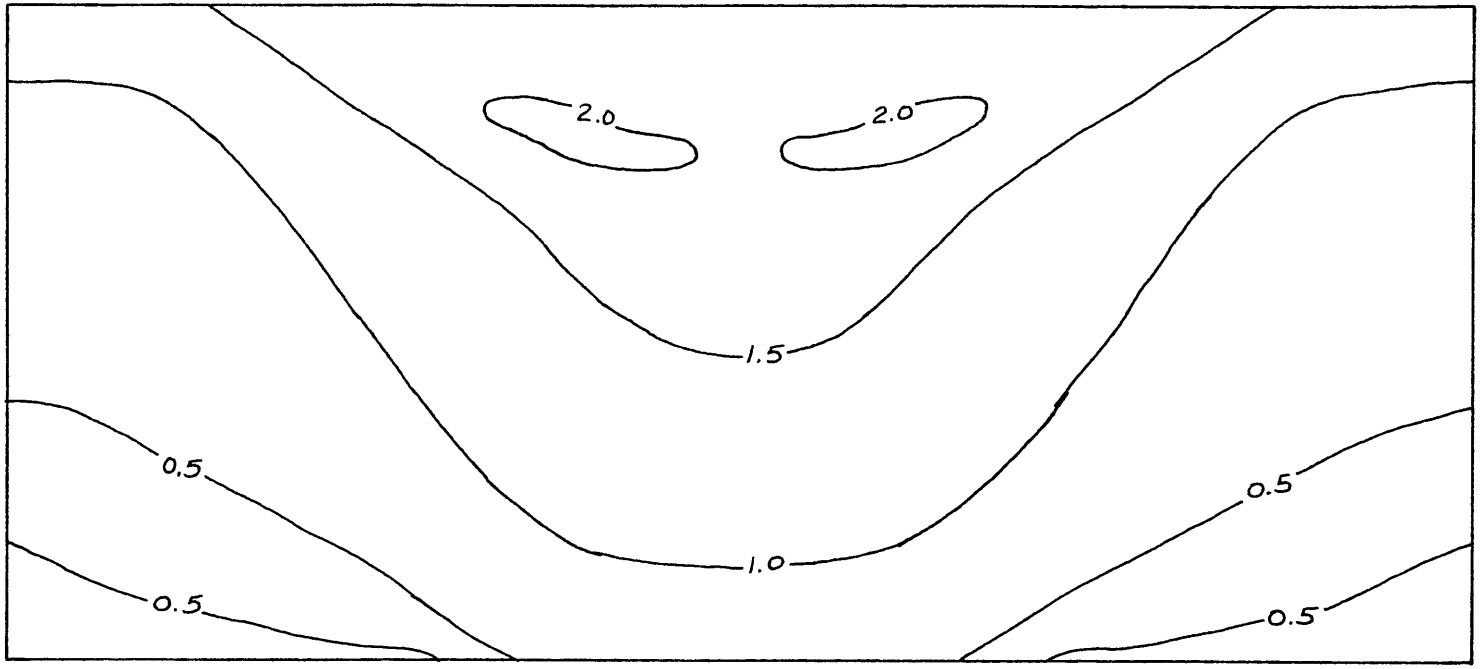

Fig. 6.22 Same as Fig. 6.18. R = 0.5, Min ω_c^2 = 0.20.

for $R_0 = .75$. Fig. 6.21 shows ω_c^2 positive everywhere, but the curve for $R_0 = .75$ in Fig. 6.16 shows that this case is unstable. For $R_0 = .50$, ω_c^2 is again positive everywhere in Fig. 6.22 and the corresponding curve in Fig. 6.16 shows no growth up to ~ 30 hours. After this time the energy begins to grow slowly, an unusual result. We see in Fig. 6.18 ($R_0 = 1.50$) that the area over which ω_c^2 is negative increases with R_0 and that some regions where ω_c^2 was negative (Fig. 6.19) are no longer so. This is because in this region both factors in ω_c^2 are negative. Therefore if the curvature is large enough, it is possible to have a stable region, even though the absolute vorticity is negative. If we can assume that ω_c^2 determines the stability of the flow, then the dependence on R_0 is clear.

In Fig. 6.17, we see that the dependence of E on $\mathcal{E}$ is very weak and in a sense opposite to that expected. We see that for the larger values of $\mathcal{E}$, which should minimize the stabilizing effect of gravity, the flow is more stable after about 60 hours. We also see that for $\mathcal{E}$ large enough the instability is little affected by increasing $\mathcal{E}$ any further.

VII. CONCLUSIONS

As we have seen in Chapter VI, anticyclonic curvature plays an important role in producing instabilities in curved flow. However, we have also learned that the simple measure of instability given by Eqn 5.2 is inadequate to explain the results of our numerical experiments.

The major results of our numerical experiments are:

1. Instabilities are suppressed in cyclonic regions of the flow and are generated in anticyclonic regions, with maximum instability in regions of maximum curvature. (Figs. 6.4-6.14)

2. Growth rates of the instability are related to the curvature of the flow, but not in any regular manner, thus growth rates are not a monotonic function of the curvature parameter R. (Fig. 6.15)

3. There is strong correlation between the Rossby number R_0 and the growth rate of the instability, probably due to the effects of $(f + R_o \bar{\zeta})$ $(f + \frac{2 R_o V}{\rho_1})$ and $\eta^2 = \frac{R_o^2 V^2}{\rho_2^2}$. (Fig. 6.16)

4. We have seen for $R_0 = .75$ ω_c^2 is positive everywhere (Fig. 6.21) yet the flow appears to be unstable (Fig. 6.16). If we include the η^2 term in Eqn 5.13, there are regions where $(\omega_c^2 - \eta^2)$ is negative. This is a strong indication that the nonsymmetric nature of the flow is important. This conclusion is partially supported by the

experiment for $R_0 = 0.5$, where $(\omega_c^2 - \eta^2) > 0$ everywhere. This run is stable to $\sim$ 30 hours. The growth of energy after this time is not easily explained.

5. In the run with $R_0 = 1.5$, we not only have (f + c) negative, but the absolute vorticity is also negative. This gives us the peculiar situation that ω_c^2 may be positive in regions of strong curvature due to the compensating effects of these two terms. (Fig. 6.18)

The present theoretical development is lacking in several respects. First, we have proceded on the basis that $\frac{\partial}{\partial s_2} \equiv 0$. From our numerical experiments, this is a reasonable approximation in region B of Fig. 6.1. On the other hand, it may not be as good in regions where the waves are oriented along the streamlines rather than across them.

The other deficiencies in the present development are that we have not been able to explain the growth rates as a function of the parameters ε and R. A more complete analysis of the problem, including the solution of Eqn 5.26, would hopefully yield such information. At that point one could be more certain about the effect of the periodic or aperiodic components of the flow. One other method of investigating the effect of the fluctuating component would be to take a series of particles, all following the same path, at fixed time lags between each successive particle. By averaging the energy curves one could obtain a mean energy curve which might show the effect of the fluctuating components by their

absence.

As an extension of the present theoretical work in Chapter V, several problems suggest themselves. The first is the use of natural coordinates in understanding the stability of barotropic flows. If we make use of our definitions of V, $\hat{t}$, $\hat{n}$, S_1, and S_2 in Chapter V, the vector barotropic vorticity equation (4.4) becomes

$$\left(\frac{\partial}{\partial t} + R_o V \frac{\partial}{\partial S_1}\right)\zeta + R_o v \frac{\partial \bar{\zeta}}{\partial S_2} = 0 \qquad (7.1)$$

where we recall that V is now a function of both s_1 and s_2, but, for stationary flows, $\bar{\zeta} = \bar{\zeta}(s_2)$ only. Since s_2 is the cross-stream coordinate, $s_2 \propto \psi$ and, by analogy with the Rayleigh problem, the stability of the flow should be dependent on whether or not $\frac{\partial \bar{\zeta}}{\partial s_2} \propto \frac{\partial \bar{\zeta}}{\partial \psi} = 0$ somewhere in the flow. We note that the problem is somewhat more complicated by the fact that $V = V(s_1, s_2)$.

Another area for further investigation is suggested by our analysis of the circular vortex in Chapter V. In a paper published some years ago, S.D.R. Wilson (1965) suggested that parallel constant shear flow might be more unstable to perturbations with a component along the flow than to purely symmetric perturbations. Our analysis also suggests this and the problem bears further research.

A related problem is that of the "almost circular vortex". A comparatively simple, analytical problem is that

of a stationary elliptical vortex, where the streamlines are concentric ellipses having an ecentricity $\epsilon \approx 1$. One should be able to do a complete analysis of this problem to point up the effect of having a changing curvature along a path, and to see if the results are radically different from a circular vortex.

This brings us to the final point in our discussion. One often cites results valid for the symmetric circular vortex to explain phenomena associated with noncircular flows. In this case a part of the flow is usually considered to be a "piece of a circular vortex." Our present investigation, however limited in scope it may be, does emphasize that this may not be the case.

REFERENCES

Arnold, V.I., 1965: On the Condition for Non-Linear Stability of Plane Stationary Curvilinear Flows in an Ideal Fluid, Proc. (Dokl.) Acad. Sci. USSR, 162, No. 5.

Blumen, W., 1968: On the Stability of Quasi-Geostrophic Flow, J. Atmos. Sci., 25, 929-931.

Charney, J.G., 1973: Planetary Fluid Dynamics, Chpt. 2, In Dynamic Meteorology, P. Morel, ed., D. Reidel Publishing Co., Boston, 622 pp.

Dikii, L.A., 1965: On the Nonlinear Theory of the Stability of Zonal Flows, IZV., Atmospheric and Oceanic Physics, 1, 653-655.

Eckart, C., 1963: Some Transformations of the Hydrodynamic Equations, The Physics of Fluids, 6, 1037-1047.

Hildebrand, F.B., 1962: Advanced Calculus for Applications, Prentice-Hall, Inc., Englewood Cliffs, 646 pp.

Houghton, D.D. and J.A. Young, 1970: A Note on Inertial Instability, Tellus, 22, 581-583.

Ince, E.L., 1926: Ordinary Differential Equations, Dover Publications, Inc., New York, 558 pp.

Lefschetz, S., 1948 : Differential Equations: Geometric Theory, second edition, John Wiley and Sons, New York, 390 pp.

Lilly, D.K., 1965: On the Computational Stability of Numerical Solutions of Time-Dependent, Non-Linear Geophysical Fluid Dynamics Problems, Mon. Wea. Rev., 93, 11-26.

Smagorinsky, J., 1958: On the Numerical Integration of the Primitive Equations of Motion For Baroclinic Flow in a Closed Region, Mon. Wea. Rev., 86, 457-466.

Whittaker, E.T. and G.N. Watson, 1927: A Course of Modern Analysis, Cambridge University Press, London, 608 pp.

Wilson, S.D.R., 1965: Instability in a geostrophic wind with a transverse wind-speed gradient, Q. J. Royal Meteor. Soc., 91, 132-139.

APPENDIX A

We consider purely barotropic, nondivergent flow on an f-plane in a periodic channel with rigid walls at y = 0 and W. The period of the channel is L. The equation of motion for such flows is

$$q_t - \psi_y q_x + \psi_x q_y = 0 \tag{A1}$$

where the subscripts t, x, y denote differentiation with respect to that variable and q is the vorticity, $q = \nabla^2\psi + f$.

In what follows, we shall keep close to the line of derivation by Blumen (1968). We can define two functions of the flow, E and ϕ, where $\phi = \phi(q)$ is an arbitrary function of q and E is the total energy of the flow

$$E = \int_0^L \int_0^W \frac{1}{2} (\psi_x^2 + \psi_y^2) \, dx \, dy \tag{A2}$$

One can easily show that

$$\frac{\partial E}{\partial t} = \frac{1}{2} \frac{\partial}{\partial t} \int_0^L \int_0^W (\psi_x^2 + \psi_y^2) \, dx \, dy = 0 \tag{A3}$$

and

$$\frac{\partial F}{\partial t} = \frac{1}{2} \frac{\partial}{\partial t} \int_0^L \int_0^W \phi(q) \, dx \, dy = 0 \tag{A4}$$

Eqn A3 is demonstrated by integrating by parts:

$$\frac{\partial}{\partial t}\int_0^L\int_0^W \tfrac{1}{2}(\psi_x^2+\psi_y^2)\,dx\,dy = \int_0^L\int_0^W (\psi_x\psi_{xt} + \psi_y\psi_{yt})\,dx\,dy$$

$$= \int_0^L\int_0^W (\psi\psi_{xt})_x + (\psi\psi_{yt})_y\,dx\,dy - \int_0^L\int_0^W (\psi\psi_{xxt} + \psi\psi_{yyt})\,dx\,dy$$

The first integral is zero, when the respective integrations are carried out, due to the periodicity in x and the boundary condition that

$$\int_0^L \frac{\partial u}{\partial t}\,dx = 0 \quad \text{and} \quad y = 0, W,$$

which is derived from the x-momentum equation. Using Eqn A1, the remaining integral becomes

$$\int_0^L\int_0^W \psi(\psi_y q_x - \psi_x q_y) =$$

$$\int_0^L\int_0^W \{(\psi\psi_y q)_x - (\psi\psi_x q)_y - (\psi_x\psi_y q + \psi\psi_{xy} - \psi_y\psi_x q - \psi\psi_{xy} q)\}$$

$$= 0$$

using the boundary condition that $\psi_x = 0$ at y = 0, w and the periodicity in x.

In a similar manner, we can prove the validity of A4.

We now form the functional $I(\psi) = E + F$ and take its variation. We assume that for some $\psi = \bar{\psi}$ I has a minimum value and thus we shall look for the conditions under which this is true. Let

$$\psi = \bar{\psi} + \delta\psi, \quad q = \bar{q} + \delta q = \nabla^2\bar{\psi} + \nabla^2\delta\psi = \nabla^2\bar{\psi} + \delta\nabla^2\psi .$$

Taking the variation of I, we get

$$\delta I = I - \bar{I} = \int_0^L\int_0^W (\bar{\Psi}_x \delta\Psi_x + \bar{\Psi}_y \delta\Psi_y + \phi'(\bar{q})\delta q) \, dx\, dy$$
$$+ \tfrac{1}{2}\int_0^L\int_0^W [(\delta\Psi_x)^2 + (\delta\Psi_y)^2 + \phi''(\bar{q})(\delta q)^2] \, dx\, dy \qquad \text{(A5)}$$
$$+ O(\delta q^3)$$

where $\bar{I} = I(\bar{\Psi})$.

The first integral becomes

$$\int_0^L\int_0^W \{[(\bar{\Psi}\delta\Psi_x)_x + (\bar{\Psi}\delta\Psi_y)_y] + \phi'(\bar{q})\delta q - \bar{\Psi}\delta\Psi_{xx} - \bar{\Psi}\delta\Psi_{yy}\} \, dx\, dy$$
$$= -\int_0^L\int_0^W [\bar{\Psi} - \phi'(\bar{q})] \delta q \, dx\, dy \; . \qquad \text{(A6)}$$

We have assumed in deriving A6 that the variations are periodic in x and vanish at y = 0, W. $I(\Psi)$ has an extremum if its first variation, given by Eqn A6, vanishes. This is true for all δq if and only if

$$\bar{\Psi} - \phi'(\bar{q}) = 0 \qquad \text{(A7)}$$

This implies that

$$\bar{\Psi} = \frac{\partial\phi}{\partial\bar{q}} \quad \text{or} \quad \phi(\bar{q}) = \int \bar{\Psi} \, d\bar{q}$$

which is to say that $\bar{\Psi} = \bar{\Psi}(\bar{q})$. This implies that a sufficient condition for an extremum of $I(\Psi)$ is that $\frac{\partial\bar{q}}{\partial t} \equiv 0$ i.e. that we have a steady-state solution for the vorticity

equation A1. It is easily shown by substituting $\bar{\Psi} = \bar{\Psi}(\bar{q})$ into Eqn A1 that this is the case.

If we now assume that $\delta q << 1$, we can neglect terms of $O(\delta q^3)$ and higher, and the second variation is positive, implying $I(\bar{\Psi})$ is a minimum. if

$$(\delta \Psi_x)^2 + (\delta \Psi_y)^2 + \frac{\partial \bar{\Psi}}{\partial \bar{q}} (\delta q)^2 \geq 0$$

over the entire domain. This is guaranteed if

$$\frac{\partial \bar{\Psi}}{\partial \bar{q}} \geq 0 \qquad \text{everywhere.}$$

This is a sufficient condition for stability.

APPENDIX B

In this section we shall outline the finite differencing approximations to Eqs 4.3b and the procedures used to integrate these difference equations. We write Eqs 4.3b schematically, dropping the " ^ " notation for the perturbation quantities

$$\frac{\partial u}{\partial t} = Fu$$

$$\frac{\partial v}{\partial t} = Fv \qquad \text{(B.1)}$$

$$\frac{\partial h}{\partial t} = Fh$$

where

$$Fu = -R_o \bar{\mathbf{V}} \cdot \nabla u + v - \frac{1}{\varepsilon R_o (1+\gamma)} \frac{\partial h}{\partial x} - R_o \left[u \frac{\partial \bar{u}}{\partial x} + v \frac{\partial \bar{u}}{\partial y} \right] \qquad \text{(B.2a)}$$

$$Fv = -R_o \bar{\mathbf{V}} \cdot \nabla v - u - \frac{1}{\varepsilon R_o (1+\gamma)} \frac{\partial h}{\partial y} - R_o \left[u \frac{\partial \bar{v}}{\partial x} + v \frac{\partial \bar{v}}{\partial y} \right] \qquad \text{(B.2b)}$$

$$Fh = -R_o \bar{\mathbf{V}} \cdot \nabla h - R_o \left(\frac{\partial u}{\partial x} + \frac{\partial v}{\partial y} \right) \qquad \text{(B.3c)}$$

The variable h in these equations has been rescaled by the factor $\varepsilon R_o (1+\gamma)$ for reasons inherent in the evolution of our numerical model.

For our time differencing scheme, we have chosen the Adams-Bashforth method. The leap-frog scheme was considered,

but the instabilities associated with it add more complications to the integration procedure than we wished to contend with. The Adams-Bashforth scheme has been shown to be (theoretically) slightly unstable (see Lilly (1965)) but our experience shows that this is not a problem. We then write the finite difference analogue of Eqs B.1

$$u^{n+1} = u^n + \frac{\Delta t}{2}\left[3Fu^n - Fu^{n-1}\right]$$

$$v^{n+1} = v^n + \frac{\Delta t}{2}\left[3Fv^n - Fv^{n-1}\right] \qquad \text{(B.3)}$$

$$h^{n+1} = h^n + \frac{\Delta t}{2}\left[3Fh^n - Fh^{n-1}\right]$$

where n refers to the values at time $t = n\Delta t$ and Δt is the time step.

In order to compute the finite difference analogues of Eqs B.2, we use a staggered grid pictured in Fig. B.1. The variables are arranged so that $v_{i1} = v_{iJMAX} = 0$, where j = 1 and j = JMAX coincide with the walls. Since the channel is periodic with period L_x we let the variables at $i = 1$ equal those at $i = IMAX$ and add enough additional points in the x-direction to overlap the ends. We may then write the finite difference approximations to Eqs B.2

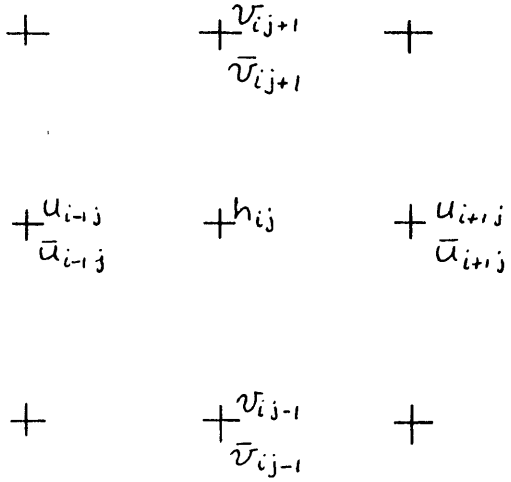

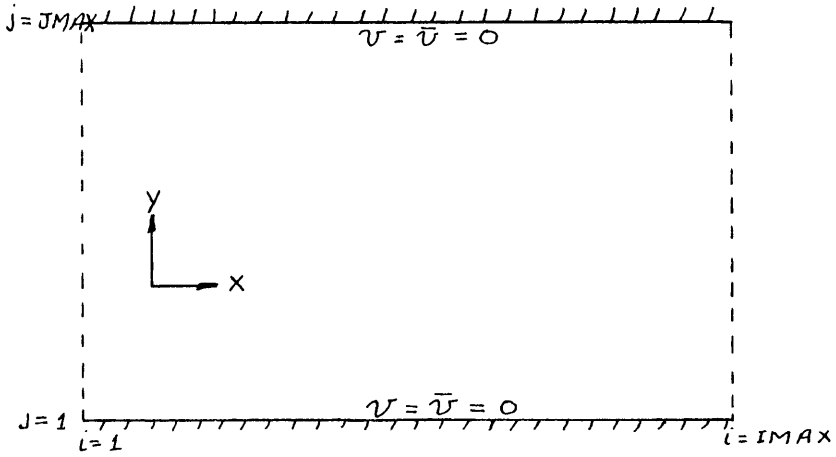

Fig. B.1 Arrangement of variables on the finite differencing grid (top figure). Relation of grid to channel (bottom figure).

$$Fh_{ij} = c_h \{ \bar{u}_{i+1j}(h_{i+2j} + h_{ij}) - \bar{u}_{i-1j}(h_{i-2j} + h_{ij})$$
$$+ \bar{v}_{ij+1}(h_{ij+2} + h_{ij}) - \bar{v}_{ij-1}(h_{ij-2} + h_{ij})$$
$$+ 2[u_{i+1j} - u_{i-1j} + v_{ij+1} - v_{ij-1}] \}$$

$$Fu_{ij} = c_u \{ (\bar{u}_{i+2j} + \bar{u}_{ij})(u_{i+2j} + u_{ij}) - (\bar{u}_{i-2j} + \bar{u}_{ij})(u_{i-2j} + u_{ij})$$
$$+ (\bar{v}_{i+1j+1} + \bar{v}_{i-1j+1})(u_{ij+2} + u_{ij}) - (\bar{v}_{i+1j-1} + \bar{v}_{i-1j-1})(u_{ij-2} + u_{ij})$$
$$+ (v_{i+1j+1} + v_{i-1j+1})(\bar{u}_{ij+2} + \bar{u}_{ij}) - (v_{i+1j-1} + v_{i-1j-1})(\bar{u}_{ij-2} + \bar{u}_{ij})$$
$$- 2[u_{ij}(\bar{v}_{i+1j+1} + \bar{v}_{i-1j+1} - \bar{v}_{i+1j-1} - \bar{v}_{i-1j-1})$$
$$+ \bar{u}_{ij}(v_{i+1j+1} + v_{i-1j+1} - v_{i+1j-1} - v_{i-1j-1})] \} \qquad \text{(B.4)}$$
$$+ \frac{1}{4}\{ v_{i+1j+1} + v_{i-1j+1} + v_{i+1j-1} + v_{i-1j-1} \}$$
$$+ c_{uh}(h_{i+1j} - h_{i-1j})$$

$$Fv_{ij} = c_u \{ \tfrac{1}{2}(\bar{u}_{i+1j+1} + \bar{u}_{i-1j+1} + \bar{u}_{i+1j-1} + \bar{u}_{i-1j-1})(v_{i+2j} - v_{i-2j})$$
$$+ \tfrac{1}{2}(u_{i+1j+1} + u_{i-1j+1} + u_{i+1j-1} + u_{i-1j-1})(\bar{v}_{i+2j} - \bar{v}_{i-2j})$$
$$+ (v_{ij+2} + v_{ij})(\bar{v}_{ij+2} + \bar{v}_{ij}) - (v_{ij-2} + v_{ij})(\bar{v}_{ij-2} + \bar{v}_{ij}) \}$$
$$- \frac{1}{4}\{ u_{i+1j+1} + u_{i-1j+1} + u_{i+1j-1} + u_{i-1j-1} \}$$
$$+ c_{uh}(h_{ij+1} - h_{ij-1})$$

where $C_{uh} = \frac{-1}{2\varepsilon(1+\gamma)\Delta X}$, $C_u = \frac{-R_o}{8\Delta X}$ and $C_h = 2C_u$. We note that the advective terms are written in flux form wherever possible. This adds some complication to the calculations but ensures that the perturbation is advected by the basic state without introducing spurious energy sources. In calculating Fu_{ij} , we must modify the equation slightly near the rigid walls, the scheme as written above requires values outside the grid. We merely recall that v and $\bar{v}$ are identically zero on the walls and omit those terms from Fu_{ij} .

The Courant-Friedrichs-Lewy stability criterion for is determined in our model by using the maximum fluid particle speed U rather than the gravity wave phase speed $C_g = U/R_o\varepsilon$. In our model $R_o \sim O(1)$ and $\varepsilon \geq 50$, therefore $C_g << U$ and a suitable Δt is determined from

$$\Delta t \leq \frac{\Delta X}{U}$$

In our model ΔX = 50 km and $U \sim fL = 10^{-4}$ sec^{-1} x 10^3 km. Thus $\Delta t \leq$ 8 min. In our computations we have taken Δt = 5 min.